ORIGINAL RESEARCH

Nkx2-5 Is Expressed in Atherosclerotic Plaques and Attenuates Development of Atherosclerosis in Apolipoprotein E–Deficient Mice

Meng Du, MD, PhD;* Xiaojing Wang, MD;* Xin Tan, PhD; Xiangrao Li, MD; Dandan Huang, MD; Kun Huang, MD, PhD; Liu Yang, MD, PhD; Fengxiao Zhang, MD, PhD; Yan Wang, MD, PhD; Dan Huang, MD, PhD;† Kai Huang, MD, PhD†

***Background*—**NK2 homeobox 5 (Nkx2-5) is a cardiac homeobox transcription factor that is expressed in a broad range of cardiac sublineages. Embryos lacking Nkx2-5 are nonviable attributed to growth retardation and gross abnormalities of the heart. However, the role of Nkx2-5 in atherosclerosis remains elusive. This study aims to elucidate the specific functions of Nkx2-5 during atherogenesis and in established atherosclerotic plaques.

***Methods and Results*—**Two types of atherosclerotic lesions were created in ApoE$^{-/-}$ mice through 2 different dietary manipulations. Mice fed a standard chow diet were sacrificed at 20 weeks old, a time point at which mice developed early-stage atherosclerotic lesions. The other half of mice were fed a western diet from 6 to 22 weeks old and then sacrificed. These mice demonstrated advanced atherosclerosis. No Nkx2-5 was detected in normal arteries; however, it was abundantly present in the intima of atherosclerotic lesions and localized in macrophages and smooth muscle cells. Adenovirus gene transfer of Nkx2-5 markedly ameliorated and stabilized the atherosclerotic plaques, and knockdown of Nkx2-5 significantly exacerbated the disease. Molecular studies indicated that expression of specific members of matrix metalloproteinases and tissue inhibitor of metalloproteinases, which play a crucial role in the progression of atherosclerosis, were directly regulated by Nkx2-5. Furthermore, we demonstrated that the compromised endothelial function, which was considered as a hallmark of early atherosclerosis, could be improved by Nkx2-5 gene transfer.

***Conclusions*—**Nkx2-5 exerts antiatherogenic effects, which may partly be attributed to regulation on matrix metalloproteinases and tissue inhibitor of metalloproteinases, thus stabilizing atherosclerotic plaque; besides, it improves endothelial function by inhibiting leukocyte adhesion to the endothelium. **(*J Am Heart Assoc*. 2016;5:e004440 doi: 10.1161/JAHA.116.004440)**

Key Words: atherosclerosis • matrix metalloproteinases • NK2 homeobox 5 • plaque stability

NK2 homeobox 5 (Nkx2-5) is a cardiac homeobox transcription factor that is expressed in a broad range of cardiac sublineages, from the early committed cardiac progenitors through the adult cardiomyocytes, and plays a pivotal role in the regulation of cardiac, vascular, and hematopoietic lineages.[1–7] The human gene, NKX2-5, is, to date, the most commonly mutated single gene in congenital heart disease, accounting for 1% to 4% of specific malformations, including atrial septal defect, double-outlet right ventricle, and a complex congenital condition arising from stenosis of the pulmonary artery termed tetralogy of Fallot.[8–11] Studies in mice show that Nkx2-5 is required for specification and spatial definition of chamber myocardium and for formation and maintenance of elements of the conduction system.[4,5,12–14]

Whereas the majority of research on Nkx2-5 is focused on its role in heart formation, recent studies have provided new insight into certain relevance of Nkx2-5 to many other pathophysiological conditions, such as early-onset and severe preeclampsia, thyroid dysgenesis, keratinocyte differentiation, and acute T-lymphoblastic leukemia.[15–20] These studies, although limited, unveiled a novel role of Nkx2-5 as a broad-acting regulatory component beyond cardiogenesis.

From the Department of Cardiology (M.D., X.W., X.T., X.L., Dandan H., Kun H., L.Y., F.Z., Y.W., Dan H., Kai H.) and Clinic Center of Human Gene Research (M.D., X.W., X.T., X.L., Dandan H., Kun H., L.Y., F.Z., Y.W., Dan H., Kai H.), Union Hospital, Tongji Medical College, Huazhong University of Science and Technology, Wuhan, China.

Accompanying Tables S1 through S4 and Figures S1 through S6 are available at http://jaha.ahajournals.org/content/5/12/e004440/DC1/embed/inline-supplementary-material-1.pdf

*Dr Du and Dr Xiaojing Wang contributed equally as co-first authors.

†Dr Dan Huang and Dr Kai Huang contributed equally as co-senior authors.

Correspondence to: Kai Huang, MD, PhD, Department of Cardiology, Union Hospital, Tongji Medical College, Huazhong University of Science and Technology, 1277 Jiefang Ave, Wuhan 430000, China. E-mail: unionhuang@163.com

Received August 9, 2016; accepted October 28, 2016.

In the present study, we showed that expression of Nkx2-5 was increased in atherosclerotic lesions of humans and ApoE$^{-/-}$ mice. Nkx2-5 gene transfer markedly ameliorated atherosclerosis, with a diminished lesion area and a more-stable plaque phenotype, and knockdown of Nkx2-5 significantly exacerbated the disease. Then, we investigated the mechanisms whereby Nkx2-5 protects against atherosclerosis through its multiple actions in macrophages, smooth muscle cells, and endothelial cells.

Material and Methods

Human Atherosclerotic Tissues

Twelve human atherosclerotic lesions were collected from patients undergoing carotid endarterectomy at Wuhan Union Hospital. Ten internal mammary arteries and 14 saphenous veins obtained from patients undergoing coronary artery bypass surgery were used as nonatherosclerotic control arteries. Written informed consent was obtained from all participants according to the declaration of Helsinki. The investigations were approved by the Ethical Committee of Huazhong University of Science and Technology.

Immunofluorescence

Immunofluorescence on human carotid artery sections and mice aortic sinus sections was performed as described.[21,22] Briefly, for double staining, sections were incubated with mouse anti-Nkx2-5 antibody (sc-376565X; Santa Cruz Biotechnology, Santa Cruz, CA), together with rabbit anti-F4/80 antibody (ab100790; Abcam, Cambridge, MA), anti-α-SMA (alpha-smooth muscle actin) antibody (ab124964; Abcam), or anti–von Willebrand factor (vWF) antibody (ab9378; Abcam) at 4°C overnight, followed by a 30-minute incubation with secondary antibody conjugated to Alexa Fluor 568 (red) and Alexa Fluor 488 (green) (Molecular Probes, Inc., Eugene, OR). Signals of individual and merged images for antigen detection were performed using a fluorescence microscope (Olympus, Tokyo, Japan) and AxioVision (version 4.8; Carl Zeiss GmbH, Jena, Germany) software.

Generation of Recombinant Adenovirus

Replication-defective recombinant adenovirus carrying the entire coding sequence of Nkx2-5 (Ad-Nkx2-5) was constructed with the Adenovirus Expression Vector Kit (Takara Bio Inc., Kusatsu, Japan). An adenovirus-only–containing green fluorescence protein (GFP) was used as a negative control (Ad-EV). To generate adenovirus expressing shRNA against Nkx2-5 (Ad-shNkx2-5), 3 siRNAs for mouse Nkx2-5 were designed and the one with the optimal knockdown efficiency was chosen to create shRNA and then recombined into adenoviral vectors. The target sequence is as follows: GCTTCAAGCAACAGCGGTA. The negative control adenovirus was designed to express nontargeting "universal control" shRNA (Ad-shNC). Amplification and purification of recombinant adenovirus was performed according to the manufacturer's instructions (Takara Bio).

Animals

Six-week-old male C57BL/6 ApoE$^{-/-}$ mice were bred and maintained under conventional housing conditions in our animal facility. These mice were divided into 8 groups (n=16 for every group). Half of them were fed a standard chow diet until sacrificed at 20 weeks old, a time point at which mice developed early-stage atherosclerotic lesions. The other 4 groups were fed a Western diet from 6 to 22 weeks old, and then the mice were sacrificed. These mice demonstrated advanced atherosclerosis. Four weeks before euthanization, animals were anesthetized with pentobarbital sodium (50 mg/kg, intraperitoneally, P3761; Sigma-Aldrich, St. Louis, MO), and either Ad-EV, Ad-Nkx2-5, Ad-shNC, or Ad-shNkx2-5 (5×10^9 plaque-forming units/mouse) was injected directly into the left ventricle of mice from each group fed chow diet or Western diet, respectively. Handling of animals was in accord with institutional guidelines.

Histological Analysis and Quantification of Atherosclerotic Lesions

Mice were fasted for 4 hours and then anesthetized. Atherosclerosis assays were performed at the indicated times of sacrifice. Lesion areas of thoracoabdominal aorta were determined by en face Oil Red O staining as described.[23] Aortas were dissected longitudinally with an extremely fine Vanna microscissor and pinned flat on a black wax surface with 0.2-mm-diameter stainless steel pins. Pinned aortas were stained with Oil Red O, and images were captured with a standard digital camera. For microscopic evaluation of the aortic sinus lesions, hearts were fixed in 4% PFA and cryopreserved in 15% sucrose and then 30% sucrose. After being embedded in optimum cutting temperature compound (Sakura Finetek, Torrance, CA), hearts were cryosectioned and 6-μm sections were collected at 80-μm intervals, starting at a 100-μm distance from the appearance of the aortic valves. Aortic sinus sections were stained for lesion areas with Oil Red O, morphology with hematoxylin and eosin (HE), collagen content with Masson's trichrome staining (Masson), and elastic fibers with elastica van Gieson staining (EVG). The relative content of macrophages, smooth muscle cells, adhesion molecules, matrix metalloproteinases (MMPs), and tissue inhibitor of metalloproteinases (TIMPs) were detected

by immunohistochemistry. Frozen serial sections were treated with 0.3% H_2O_2 in PBS to block endogenous peroxidase activity, followed by blocking in 4% BSA (Sigma-Aldrich). Primary antibodies were specific for the following: F4/80 (ab100790; Abcam); α-SMA (ab124964; Abcam); vWF (ab9378; Abcam); MMP2 (AP51352; Abgent); MMP9 (AP6214a; Abgent, San Diego, CA); MMP3 (AP51354 Abgent), MMP8 (AP51356; Abgent); MMP14 (AP6198a; Abgent); TIMP1 (ab86482, Abcam), E-selectin (ab18981; Abcam); and vascular cell adhesion molecule-1 (VCAM1; ab134047; Abcam). All sections were stained with biotinylated secondary antibodies and detected using ABC reagents (Vector Laboratories, Burlingame, CA). Collected images were quantitated by quantitative morphometry using the Image Pro Plus program. Lesion areas were determined by calculating the mean lesion area of the 4 sections at 80-μm intervals. For evaluation of the relative content of the stained constituents, we determined the percentage of blue (collagen on Masson's trichrome staining) and diaminobenzidine-positive (immunohistochemistry) areas to the total plaque areas. Fibrous caps were defined as the vascular smooth muscle cell (VSMC)- and collagen-rich area overlying the cholesterol-rich, matrix-poor, and acellular regions of the necrotic cores. In EVG-stained sections, the number of ruptures (ie, discontinuities or fractures) of the elastic lamina was determined.

In Situ Zymography

To detect and localize gelatinolytic activity of MMPs in aortic sinus, in situ zymography was carried out as described previously.[24] Briefly, 100 μg/mL of fluorescein-conjugated dye-quenched (DQ) gelatin (Molecular Probes) was mixed with 0.2% agarose melted in reaction buffer (50 mmol/L of Tris-HCl [pH 7.5] 0.15 mol/L of NaCl, 5 mmol/L of $CaCl_2$, and 0.2 mmol/L of sodium azide). Aortic sinus sections were incubated with the reaction mixture prepared above for 24 hours at 37°C in a moist dark chamber and then rinsed 3 times in PBS and mounted in Vectashield mounting medium (Vector Laboratories) for fluorescence microscopy. When DQ gelatin is cleaved by gelatinolytic activity, fluorescent peptides are released that are visible against a weakly fluorescent background.

Cell Culture

Peripheral blood mononuclear cells (PBMCs) were prepared on a Ficoll-Hypaque density gradient centrifugation. $CD14^+$ cells were obtained through positive selection by $CD14^+$ micromagnetic beads according to the manufacturer's instructions (Miltenyi Biotec, Bergisch Gladbach, Germany). Then, monocytes were differentiated in complete RPMI-1640 medium supplemented with recombinant human macrophage colony-stimulating factor (50 ng/mL; R&D Systems, Minneapolis, MN) for an additional 6 days before following study. Human primary aortic smooth muscle cells (HASMCs; ATCC PCS-100-012; American Type Culture Collection [ATCC], Manassas, VA) and human primary aortic endothelial cells (HAECs; ATCC PCS-100-011; ATCC) were cultured according to the manufacturer's instructions. Cells were used for experiments at passages 3 to 8.

Western Blot

Cells or tissues were homogenized in ice-cold suspension buffer supplemented with a proteinase inhibitor cocktail (Sigma-Aldrich) as described previously.[25] Protein concentrations were determined using the BCA Protein assay kit (Thermo Scientific, Waltham, MA). Equal amounts of protein were fractionated by SDS polyacrylamide gels, followed by immunoblotting with the following primary antibodies: MMP1 (AP51345; Abgent); MMP2 (AP51352; Abgent); MMP3 (AP51354; Abgent); MMP7 (ALS11637; Abgent); MMP8 (AP51356; Abgent); MMP9 (AP6214a; Abgent); MMP10 (AP50649; Abgent); MMP11 (AP51347; Abgent); MMP12 (AP6196a; Abgent); MMP13 (AP51348; Abgent); MMP14 (AP6198a; Abgent); TIMP1 (sc-21734; Santa Cruz Biotechnology); TIMP2 (sc-365671; Santa Cruz Biotechnology); TIMP3 (sc-373839; Santa Cruz Biotechnology); TIMP4 (sc-9375; Santa Cruz Biotechnology); intracellular adhesion molecule-1 (ICAM1; ab124759; Abcam); VCAM1 (ab134047; Abcam), E-selectin (ab18981; Abcam), P-selectin (ab178424; Abcam); nuclear factor kappa B (NF-κB) Pathway Sampler Kit (9936; Cell Signaling Technology [CST], Danvers, MA); and phospho-MAPK (mitogen-activated protein kinase) Family Antibody Sampler Kit (9910; CST). Membranes were then incubated with peroxidase-conjugated secondary antibody, and specific bands were detected with a Bio-Rad (Hercules, CA) imaging system.

Real-Time Reverse-Transcriptase Polymerase Chain Reaction

Total RNA was extracted from cells with the use of TRIzol reagent (D9108A; Takara Bio). RNA was reverse-transcribed using the RNA PCR Kit (RR036A; Takara Bio). Quantitative polymerase chain reaction (PCR) amplification was performed with an ABI PRISM 7900 Sequence Detector system (Applied Biosystem, Foster City, CA), according to the manufacturer's instructions. The real-time PCR primer sequences are shown in Table S1.

Adhesion Assay

Adhesion assay was performed using Endothelial Cell Adhesion Assay Kit (ECM645; Bioscience Research Reagents

[formerly Chemicon], Billerica, MA) according to the kit instructions, with modifications. HAECs (PCS-100-011; ATCC) were grown on chamber slides where adhesion assay was performed. Cells were infected with Ad-Nkx2-5 or Ad-EV, followed by treating with tumor necrosis factor alpha (TNFα; 10 ng/mL) for 6 hours. Fresh adult human PBMCs (PCS-800-011; ATCC) were labeled with calcein acetomethoxy (AM) dye: PBMCs were pelleted at 240*g* for 10 minutes, resuspended in 1 mL of culture medium with 2.5 μmol/L of calcein AM from the kit, and incubated at 37°C (5% CO_2) for 30 minutes. PBMCs were then washed 3 times with HAEC media and added to HAEC cells (150 000 labeled PBMCs per chamber). PBMCs were allowed to settle down and adhere to HAECs for 1 hour. Then, unbound PBMCs were washed out by gentle removal and addition of culture medium in chambers 3 times. Following the washing of unbound PBMCs, HAECs with attached PBMCs were fixed for 10 minutes in 2% formaldehyde at room temperature, permeabilyzed with 0.1% Triton X-100, stained with 2.5 μg/mL of 4′,6-diamidino-2-phenylindole (DAPI; DNA stain; Invitrogen, Carlsbad, CA) and mounted with ProLong Gold antifade reagent (Invitrogen). PBMCs were identified and counted based on calcein AM green fluorescence (excitation, 495 nm; emission, 516 nm), and total number of cells was counted based on DAPI fluorescence (350-nm excitation, 470-nm emission).

Luciferase Assays

Promoters of members of MMPs and TIMPs, E-selectin, P-selectin, VCAM1, and ICAM1 were subcloned into the pGL3-Basic vector (Promega, Madison, WI) using the One Step Cloning Kit (C112-02; Vazyme Biotech Ltd., Nanjing, China). Primers and the length of PCR products (the restriction enzyme sites are not included) are demonstrated in Table S2. Luciferase reporter constructs were cotransfected with an internal control plasmid, pRL-TK (Renilla luciferase reporter plasmid; Promega), into HEK293 cells, followed by infection with Ad-Nkx2-5 or Ad-EV. Then, cells were harvested, lysed, and the luciferase activity was determined with the Dual Luciferase Reporter Assay Kit (Promega), according to the manufacturer's instruction.

Chromatin Immunoprecipitation Assay

Chromatin immunoprecipitation (ChIP) assay was performed according to instructions (CHIP assay kit; Millipore, Billerica, MA) using mouse monoclonal antibodies against Nkx2-5 (sc-376565X; Santa Cruz Biotechnology). DNA samples recovered after immunoprecipitation were subjected to PCR using primers demonstrated in Table S3. As negative controls, ChIP was performed in the presence of mouse immunoglobulin G (IgG).

Statistical Analysis

GraphPad Prism software (GraphPad Software Inc., La Jolla, CA) was used for statistical analyses. Data were normally distributed, as assessed by using the Kolmogorov–Smirnov test. Comparisons between groups were carried out using the Student *t* test. Data are presented as mean±SEM, and a value of $P<0.05$ was considered as statistically significant.

Results

Nkx2-5 Is Expressed in Human and Mice Atherosclerotic Plaque

To characterize the involvement of Nkx2-5 in atherosclerosis, we first examined expression of Nkx2-5 in several human healthy vessels (saphenous vein and internal mammary artery) and carotid atherosclerotic plaques. As double immunofluorescent staining demonstrated, Nkx2-5 was virtually undetectable in healthy arteries. However, in atherosclerotic plaque, Nkx2-5 was expressed predominantly in macrophages and smooth muscle cells that exhibited positive staining for CD68 or α-SMA, respectively. Little-to-no Nkx2-5 immunoreactivity was detected in medial smooth muscle cells beneath plaque or endothelial cells lining the lumen of the diseased vessel. But, surprisingly, a certain number of Nkx2-5 and vWF double-positive cells could be observed in the subendothelial neovascular (Figure 1A and 1B). Moreover, Nkx2-5 protein levels, as detected by western blot, were markedly increased in plaques (2 of 3 plaques contained Nkx2-5) versus control vessels (Figure 1C). Given that $ApoE^{-/-}$ mice demonstrate the atherosclerosis phenotype, we further performed immunostaining to analyze expression of Nkx2-5 in diseased $ApoE^{-/-}$ mice and normal C57BL/6 mice. Consistent with our previous findings in human atherosclerotic plaque, evident immunoreactivity for Nkx2-5 was detected in macrophages and smooth muscle cells in aortic sinus lesions of $ApoE^{-/-}$ mice, whereas normal C57BL/6 mice demonstrated no positive staining for Nkx2-5 (Figure S1A). Western blot was further conducted to determine the protein levels of Nkx2-5 in mice. As demonstrated in Figure S1B, Nkx2-5 protein was relatively abundant in heart, liver, lung, kidney, and adipose tissue, whereas it was barely detectable in spleen, aorta, and muscle. As expected, Nkx2-5 levels in aorta of $ApoE^{-/-}$ mice were increased with age, and more markedly when mice were fed with a Western diet. However, we failed to detect Nkx2-5 expression in aorta of C57BL/6 mice, even on the Western diet (Figure S1C). These results indicated that upregulation of Nkx2-5 was associated with severity of atherosclerosis rather than age or diet.

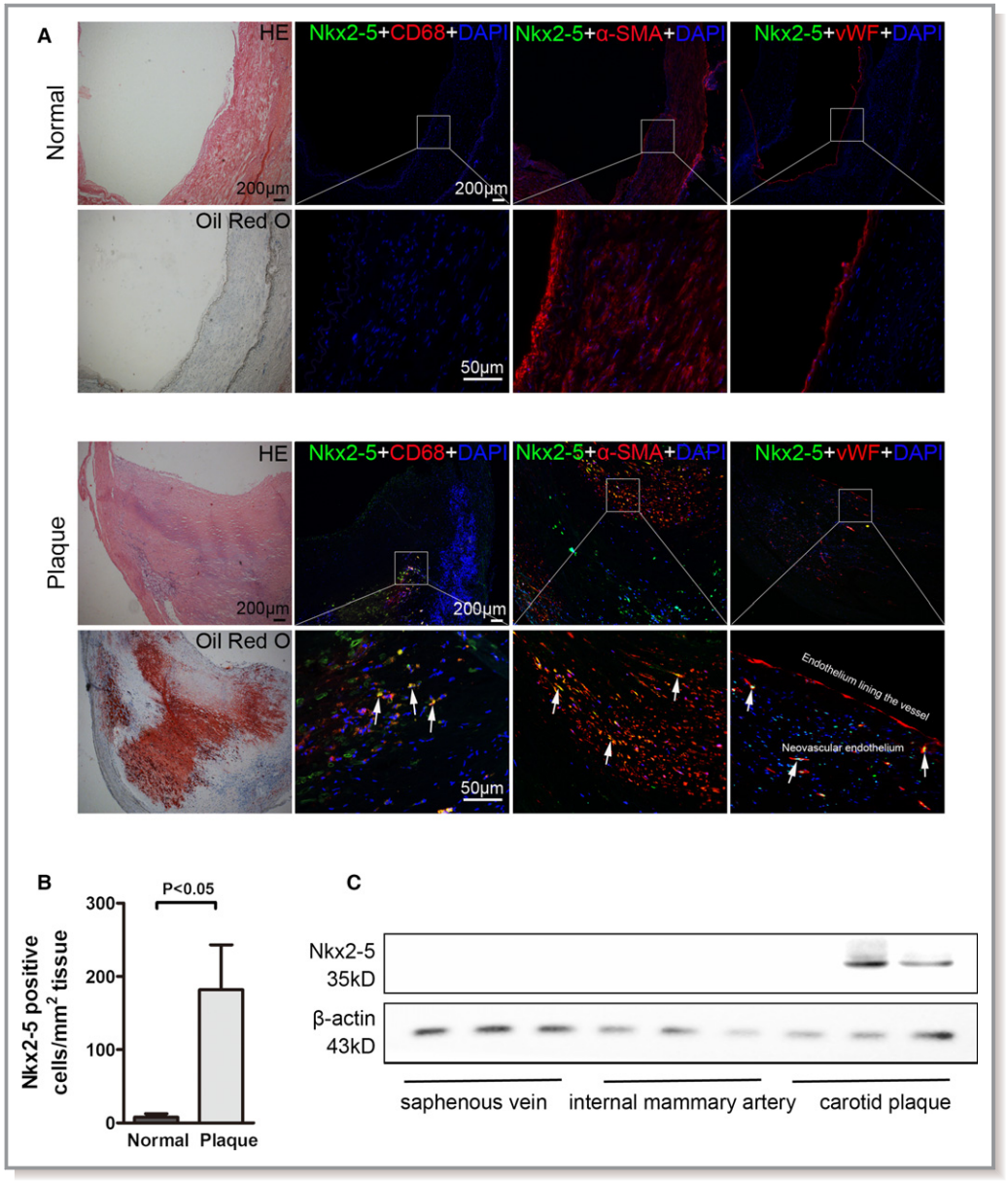

Figure 1. NK2 homeobox 5 (Nkx2-5) expression in human normal vessels and atherosclerotic plaques. A, Immunofluorescence assay of Nkx2-5 in internal mammary arteries (normal, upper) and atherosclerotic lesions of carotid arteries (plaque, lower). For colocalization analysis, sections were costained for Nkx2-5 (green) and CD68 (red, macrophage marker), α-SMA (red, smooth muscle cell marker), or von Willebrand Factor (vWF; red, endothelial marker). 4′,6-diamidino-2-phenylindole (DAPI) was used for nucleus staining (blue). Arrows indicate Nkx2-5 and cell-specific marker double-positive cells. B, Quantitative analysis of Nkx2-5-positive cells in (A). n=5 for each group. C, Western blot for Nkx2-5 expression in human control vessels (saphenous vein and internal mammary artery) and carotid atherosclerotic plaques. n=12 for atherosclerotic plaques, 10 for internal mammary artery, and 14 for saphenous vein. HE indicates hematoxylin and eosin; α-SMA, alpha-smooth muscle actin.

Evaluation of Adenovirus Infection Efficiency in Arterial Walls of Experimental Atherosclerotic Mice After Intraventricular Administration

To identify the role of Nkx2-5 in atherosclerosis, recombinant adenovirus were generated and injected directly into left ventricles of anesthetized animals by heart puncture. To evaluate the efficiency of gene transfer in aortic tissue of animals, expression of GFP in various tissues was examined by western blot and compared with that of tail vein injection. As illustrated in Figure S2A, GFP protein was detected mainly in liver and aortic tissue of mice receiving adenovirus

intraventricularly for 1 week. However, adenovirus infection efficiency in aorta was relatively low when administrated through the tail vein. Time-course experiments revealed that transgene expression in aorta was evident at 1 week and declined progressively at 2 and 4 weeks after virus administration (Figure S2B). Considering the spatial distribution and temporal variation of the transgene expression, adenovirus was administrated intraventricularly 4 weeks before mice were sacrificed, as depicted in Figure S2C. To further confirm infection efficiency, Nkx2-5 expression of aorta was examined by western blot. Whether fed a standard chow diet or a Western diet, further increase in Nkx2-5 protein was detected in aortic tissue of mice receiving Ad-Nkx2-5, which was sustained until experiment termination. Conversely, no Nkx2-5 protein was detectable in aorta from mice injected with Ad-shNkx2-5 (Figure S2D).

Effect of Nkx2-5 on Initiation and Progression of Atherosclerosis

Two types of atherosclerotic lesions (referred to as early and advanced stage) were created in ApoE$^{-/-}$ mice through 2 different dietary manipulations as previously described (Figure S2C). Four weeks before euthanization, either Ad-EV, Ad-Nkx2-5, Ad-shNC, or Ad-shNkx2-5 was delivered by intraventricular injection. Body weights and plasma lipid profiles were unaffected by Nkx2-5 gene transfer (Table S4). Proportions of CD3$^+$, CD4$^+$, or CD8$^+$ lymphocytes in spleen of animals fed a Western diet were not affected by Nkx2-5. Neither did the relative mRNA expression of certain transcription factors representative for T-cell subsets, including T-bet, GATA3, RORc, and Foxp3 (Figure S3). The lesion area that developed at the aortic sinus of Ad-Nkx2-5-treated mice fed a chow diet was decreased by 50.6%, compared to those of control littermates treated with Ad-EV, whereas the difference in lesion areas was not statistically significant between Ad-shNkx2– treated mice and Ad-shNC-treated mice (Figure 2A and 2B). For the Western diet–fed mice, which exhibited advanced lesions, the atherosclerotic lesion area in Ad-Nkx2-5-treated mice, as determined by Oil Red O staining of the thoracoabdominal aorta, was significantly decreased by 45.2% when compared to Ad-EV-treated mice, and Nkx2-5 knockdown obviously accelerated atherosclerotic plaque formation (increased by 40.3% compared to Ad-shNC-treated mice; Figure 2E and 2F). Additionally, histological evaluation showed that plaque areas in the aortic sinus were consistent with the gross observation (Figure 2C and 2D).

Effects of Nkx2-5 on Lesional Morphology of Advanced Atherosclerotic Plaque

Nkx2-5 not only affected plaque size, but also induced marked changes in morphology in ApoE$^{-/-}$ mice fed a Western diet (Figure 3). Compared with Ad-EV-treated mice, plaques of Ad-Nkx2-5-treated mice contained a relatively integral VSMC-rich fibrous cap with abundant collagen and matrix overlying small necrotic cores. Macrophage content, determined by F4/80 immunostaining, was considerably decreased and degradation of elastic fibers in tunica media could hardly be observed. However, fibrous caps were markedly thinner and collagen content was decreased in Ad-shNkx2-5-treated mice compared to their control littermates treated with Ad-shNC. Although migratory smooth muscle cells significantly increased in Ad-shNkx2-5-treated mice, they scattered throughout the lesions and tended to contribute to plaque expansion, instead of favoring fibrous cap formation. Besides, the infiltrating of macrophages and destruction of the elastic laminae were more pronounced in Ad-shNkx2-5-treated mice compared to Ad-shNC treated mice.

The MMPs are zinc-dependent proteases that play a critical role in extracellular matrix degradation, tissue remodeling, aneurysm formation, and plaque rupture. We then examined whether plaque vulnerability was related to the action of MMPs. As immunohistochemical staining demonstrated, MMP2 and MMP9 expression in atherosclerotic lesions was substantially decreased in mice treated with Ad-Nkx2-5, compared to Ad-EV-treated controls, and Ad-shNkx2-5 infection significant increased the levels of MMP2 and MMP9 (Figure 4A and 4B). Given that the mere presence of MMP proteins may not establish their catalytic capacity, we further examined MMP enzymatic activity in atherosclerotic lesions using in situ fluorescent zymography. As illustrated in Figure 4C and 4D, obvious gelatinolytic activity, demonstrated as the presence of signal for gelatinolytic product formation, was observed in aortic sinus lesions. A relative weak signal was detected in mice treated with Ad-Nkx2-5, whereas a stronger gelatinolytic activity was observed in Ad-shNkx2-5-treated mice.

Nkx2-5 Regulates the Expression of MMPs and TIMPs Directly in Human Monocyte-Derived Macrophages and HASMCs

To examine whether expression of MMPs, including MMP2 and MMP9, was directly regulated by Nkx2-5, protein levels of MMPs, as well as their main natural inhibitors, TIMPs, were quantified in human peripheral blood monocyte-derived macrophages and HASMCs using western blot. Surprisingly, compared to the Ad-EV-treated group, MMP2, MMP8, MMP9, MMP10, MMP11, and MMP14 were all remarkably downregulated in macrophages infected with Ad-Nkx2-5, along with increased expression of MMP12 and MMP13, whereas the expression of MMP1, MMP3, and MMP7 were not significantly different. For the TIMP family, TIMP1 and TIMP2 were obviously induced by Ad-Nkx2-5 transfection, whereas

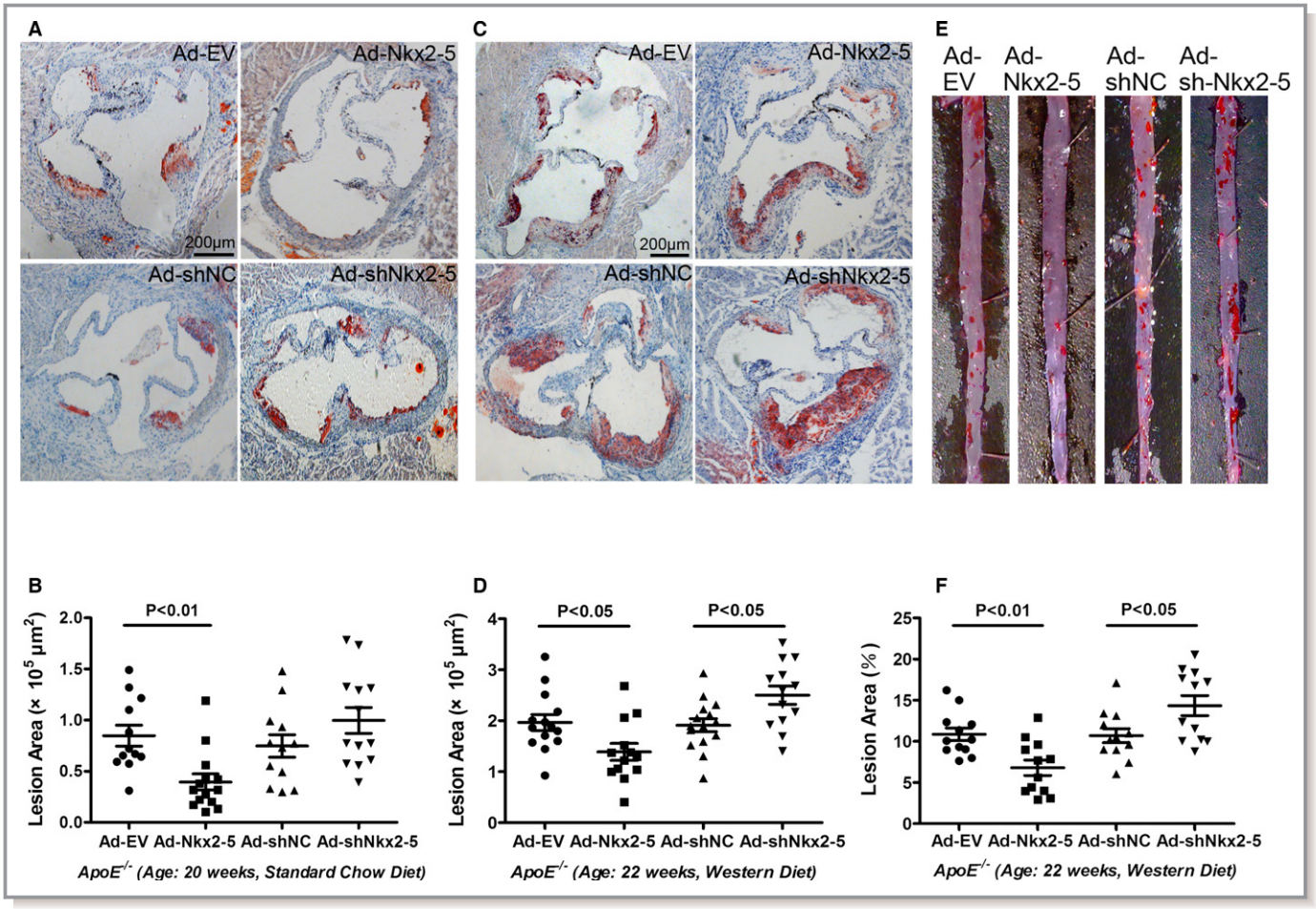

Figure 2. NK2 homeobox 5 (Nkx2-5) exerts protective effect in the initiation and progression of atherosclerosis in ApoE$^{-/-}$ mice. A and B, ApoE$^{-/-}$ mice fed a chow diet were administrated adenovirus and sacrificed at 20 weeks. Cross-sections of aortic sinus were stained with Oil Red O, and lesion areas were quantified. Data are expressed as mean±SEM (n=12 for Ad-EV, 14 for Ad-Nkx2-5, 12 for Ad-shNC, and 13 for the Ad-shNkx2-5–treated group). C and D, ApoE$^{-/-}$ mice fed a Western diet were administrated adenovirus and sacrificed at 22 weeks. Cross-sections of aortic sinus were stained with Oil Red O, and lesion areas were quantified. Data are expressed as mean±SEM (n=14 for Ad-EV, 13 for Ad-Nkx2-5, 15 for Ad-shNC, and 13 for the Ad-shNkx2-5–treated group). E and F, ApoE$^{-/-}$ mice fed a Western diet were administrated adenovirus and sacrificed at 22 weeks. Lesion areas of thoracoabdominal aorta were evaluated by en face staining with Oil Red O. Data are expressed as mean±SEM (n=12 per group).

expression of TIMP3 and TIMP4 were almost unaffected (Figure 5A and 5C). Moreover, in smooth muscle cells, the change tendency of MMPs and TIMPs was consistent with that observed in macrophages. Expression of MMP7, MMP8, MMP10, and TIMP4, however, were hardly detectable in smooth muscle cells, which was probably attributed to a very low protein level (Figure 5B and 5D).

Nkx2-5 was initially discovered as a cardiac homeobox transcription factor, which played a pivotal role in the transcriptional regulation of cardiac, vascular, and hematopoietic lineages. To explore whether Nkx2-5 could also directly regulate transcription of MMPs and TIMPs, we established the promoter-luciferase reporter constructs containing the sequences ranging from upstream 2000 base pairs (bp) to downstream 200 bp of gene transcription initiation sites. The dual luciferase reporter gene assay was conducted in HEK293 cells. As depicted in Figure 6, Nkx2-5 overexpression significantly reduced the promoter activity of MMP2, MMP8, MMP9, MMP10, MMP11, and MMP14 and also enhanced TIMP1 promoter activity. The results indicated that the specific members of this family were most likely to be the novel target genes of Nkx2-5.

To determine whether Nkx2-5 showed high enrichment in promoters of MMPs/TIMPs, ChIP was performed in human monocytic leukemia cell line (THP1)-derived macrophages. By bioinformatics analysis, several putative Nkx2-5 binding sites, which contained the consensus sequence of 5′-TNAAGTG-3′ or 5′-TTAATT-3′, were found in each MMP or TIMP promoter ranging from −2000 to +200 bp, except for TIMP4, and they are denoted as “seq-No.” in Figure S4. As expected, no significant occupancy of Nkx2-5 on the promoters was observed in cells infected with Ad-EV. However, for the Ad-

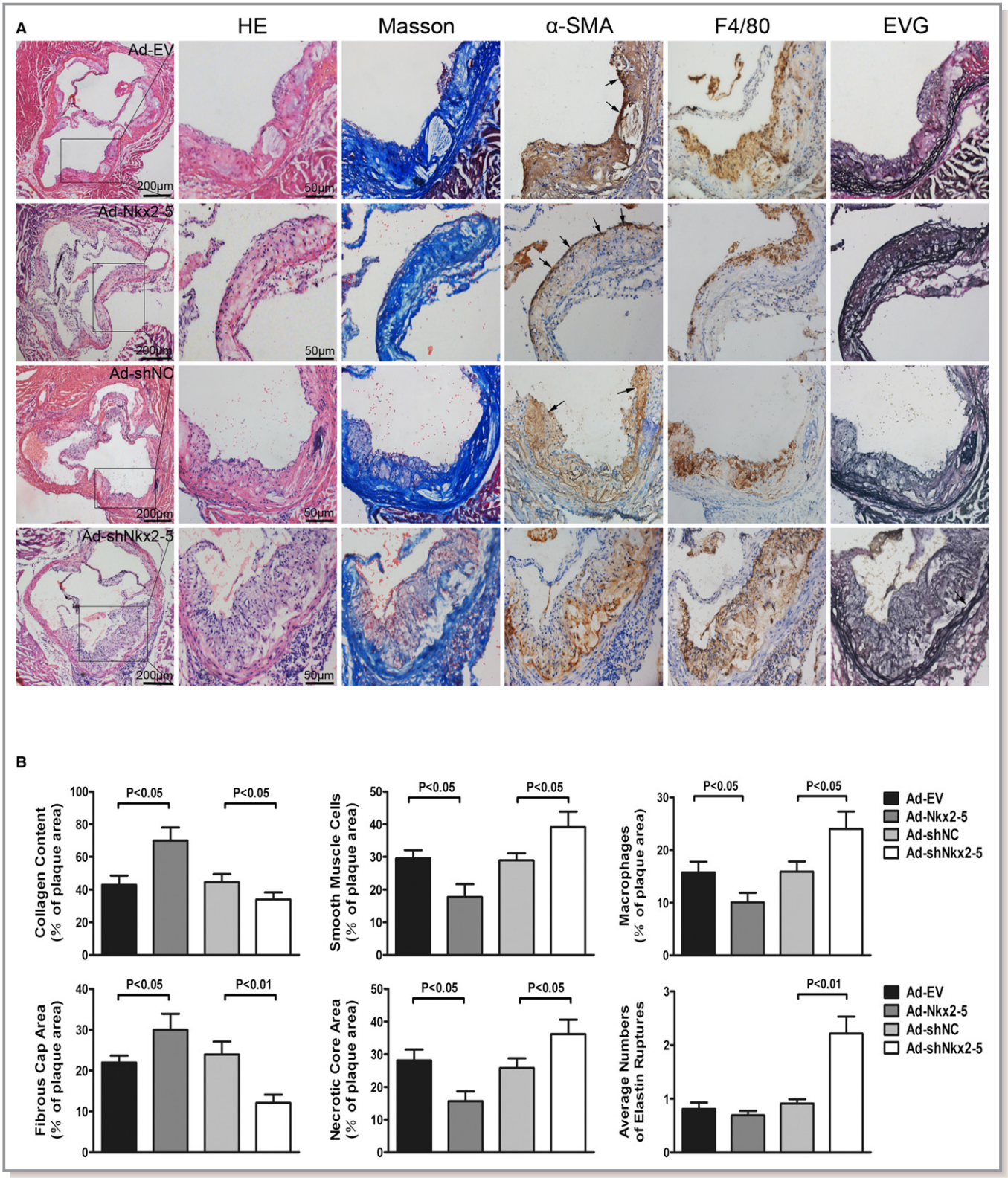

Figure 3. Histological analysis of aortic sinus lesions of ApoE$^{-/-}$ mice fed a Western diet. A, Images show representative sections of aortic sinus from each group of mice stained with hematoxylin and eosin (HE), Masson's trichrome (Masson), elastica van Gieson (EVG), anti-α-SMA antibody, and anti-F4/80 antibody. B, Collagen content, smooth muscle cells, macrophages, fibrous cap area, and necrotic core area are quantified as a percent of total plaque area. Elastic lamina destruction of the tunica media was evaluated by quantifying the ruptures of elastic fibers. Arrows in α-SMA staining panels indicate smooth muscle cells favoring fibrous caps formation, and arrows in EVG staining panels indicate ruptures of elastic fibers of tunica media. Data are expressed as mean±SEM (n=12 per group). α-SMA indicates alpha-smooth muscle actin.

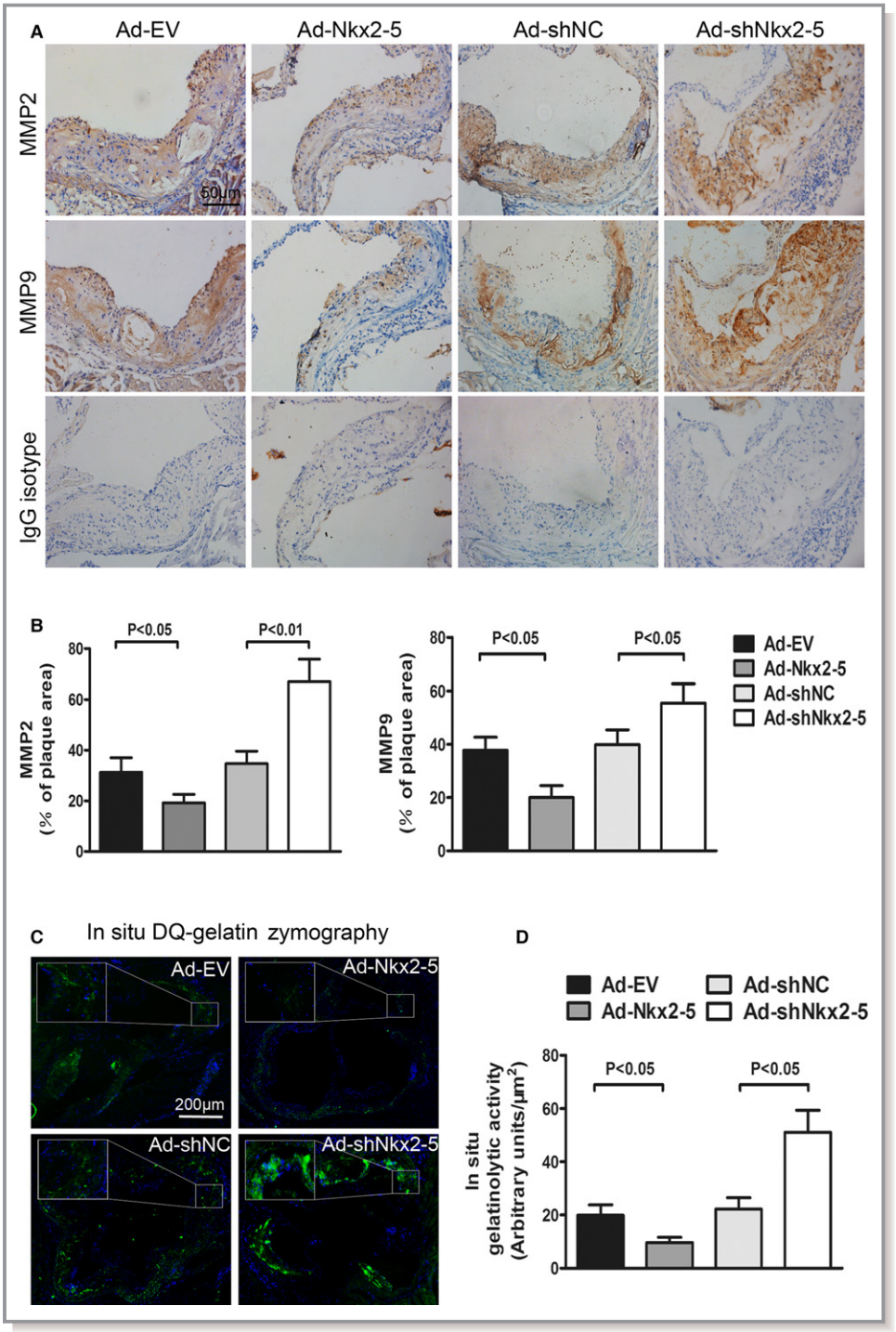

Figure 4. Effects of NK2 homeobox 5 (Nkx2-5) on MMP2/9 expression and activities in ApoE$^{-/-}$ mice fed a Western diet. A, Cross-sections of aortic sinus were immunostained with antibodies against MMP2 and MMP9. Staining with rabbit IgG isotype was used as the negative control for MMP2 and MMP9. B, Quantification of histochemical staining of MMP2 and MMP9. Positive stained areas were quantified as a percentage of total plaque area. Data are expressed as mean±SEM (n=12 per group). C, In situ zymographic analysis of MMP2/9 activities in aortic sinus. Localization of green fluorescence indicates gelatinolytic activities of MMP2 and MMP9, and 4′,6-diamidino-2-phenylindole (DAPI) was used for nucleus staining. All images were obtained under identical conditions of laser beam intensity and exposure time; representative images are displayed. D, Quantitative analysis of fluorescence intensity in (C). Data are expressed as mean±SEM (n=12 per group). DQ indicates dye-quenched; IgG, immunoglobulin G; MMP, matrix metalloproteinase.

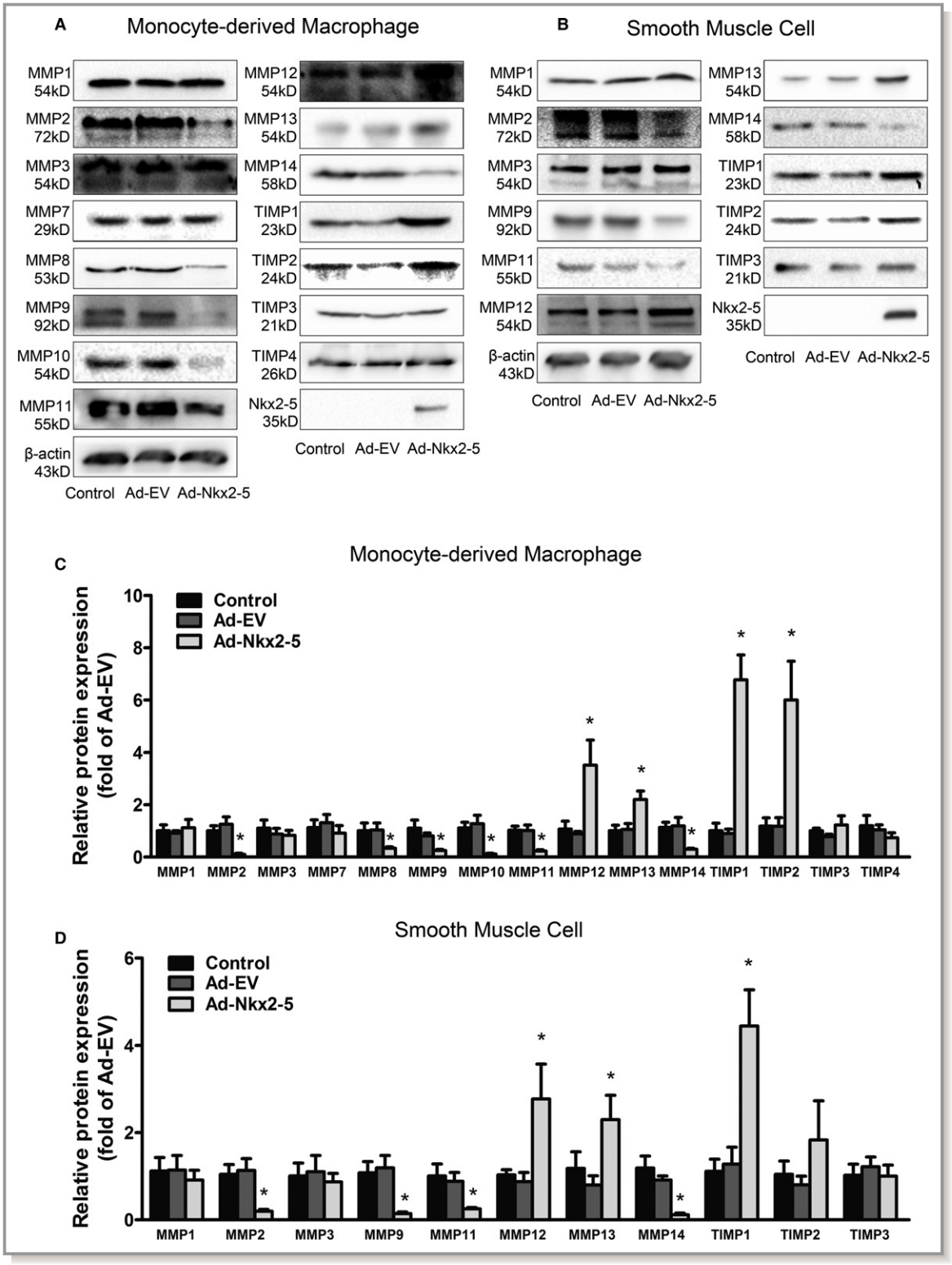

Figure 5. NK2 homeobox 5 (Nkx2-5) regulates expression of MMPs and TIMPs in human monocyte-derived macrophages and human aortic smooth muscle cells. A, Representative immunoblot for MMPs and TIMPs in human peripheral blood monocyte-derived macrophages infected with Ad-EV or Ad-Nkx2-5. B, Representative immunoblot for MMPs and TIMPs in human aortic smooth muscle cells infected with Ad-EV or Ad-Nkx2-5. C, Quantification of band density in (A). Results are expressed as fold of control group. Data represent the mean±SEM of 3 independent experiments. *P<0.05 versus Ad-EV group. D, Quantification of band density in (B). Results are expressed as fold of control group. Data represent the mean±SEM of 3 independent experiments. *P<0.05 versus Ad-EV group. MMP indicates matrix metalloproteinase; TIMP, tissue inhibitor of metalloproteinase.

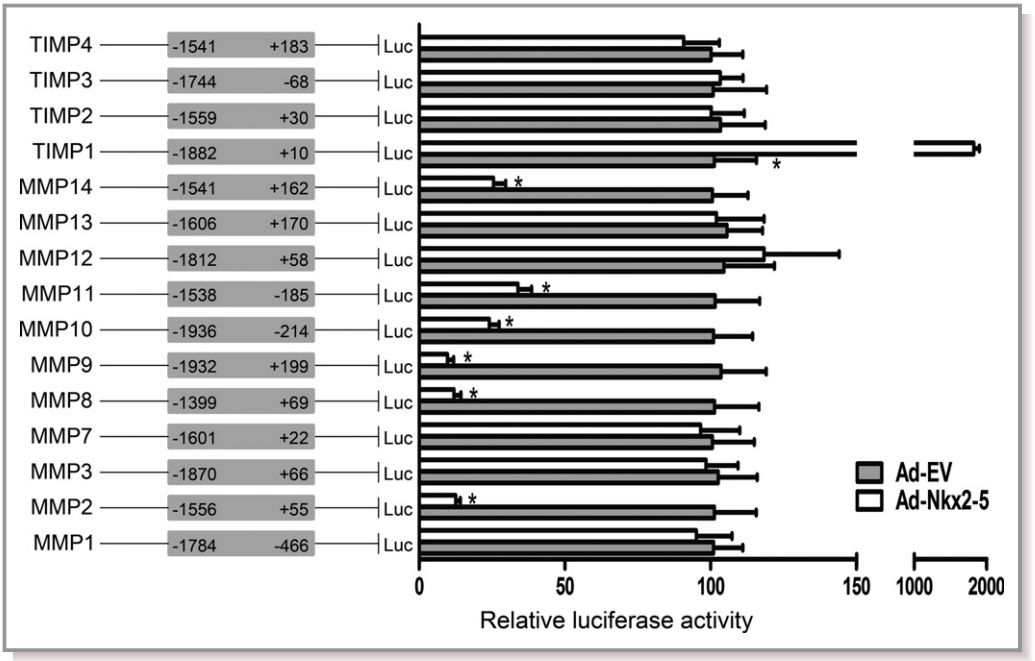

Figure 6. NK2 homeobox 5 (Nkx2-5) directly regulates MMPs/TIMPs transcription. Luciferase (Luc) reporter constructs containing promoters of MMPs or TIMPs were cotransfected with an internal control plasmid pRL-TK into HEK293 cells, followed by infection with Ad-Nkx2-5 or Ad-EV. Schematic representation in the left panel demonstrates the range of promoters, and the numbers indicate nucleotide positions relative to the transcription initiation site. The right panel demonstrates relative luciferase activities, which are expressed as a percent of values determined in the Ad-EV-treated group. Data represent the mean±SEM of 3 independent experiments. *$P<0.05$ versus the Ad-EV-treated group. MMP indicates matrix metalloproteinase; TIMP, tissue inhibitor of metalloproteinase.

Nkx2-5-treated group, Nkx2-5 enrichment in the specific binding sites of MMPs/TIMPs gene promoters was observed, including MMP2, MMP3, MMP8, MMP9, MMP10, MMP11, MMP14, and TIMP1 (Figure S4). The putative Nkx2-5 binding sites of each promoter, as well as specific PCR primers and product lengths, are demonstrated in Table S3.

Besides MMP2 and MMP9, expression of MMP3, MMP8, MMP14, and TIMP1 was also examined in the atherosclerotic lesions of ApoE$^{-/-}$ mice fed a Western diet. As expected, Nkx2-5 gene transfer significantly inhibited expression of MMP8 and MMP14 and enhanced TIMP1 expression. There was no difference in the level of MMP3 between Ad-Nkx2-5-treated mice and Ad-EV-treated mice (Figure S5).

Nkx2-5 Regulates Expression of Extra Functional Genes in Macrophages, Smooth Muscle Cells, and Endothelial Cells

Atherosclerosis is a chronic vascular inflammatory disease, with a series of cytokine-mediated interactions among multiple kinds of cells. Besides being involved in extracellular matrix remolding, whether Nkx2-5 could exhibit far-ranging effects on disease progression is still unknown. Expression of several key functional genes was detected in human peripheral blood monocyte-derived macrophages, HASMCs, and HAECs. Reverse-transcriptase PCR analysis demonstrated that macrophages infected with Ad-Nkx2-5 had significantly lower mRNA levels of the proinflammatory cytokines, interleukin (IL) 1α, IL1β, and IL18, along with upregulated IL10, a well-known anti-inflammatory cytokine. We could not ignore that Nkx2-5 also augmented expression of interferon-gamma, which could exacerbate atherosclerosis as an important activator of macrophages and inducer of adaptive immunity (Figure 7A). No appreciable changes of genes related to cholesterol metabolism and foam cell formation were observed (Figure 7A). Also, genes involved in apoptosis and phenotype transformation of smooth muscle cells were almost unaffected by Nkx2-5 except for KLF4 (Figure 7B).

Moreover, whether Nkx2-5 could be involved in regulation of endothelial functions was investigated (Figure 7C). Of note, in cultured aortic endothelial cells, Nkx2-5 exhibited a potent inhibitory effect on mRNA levels of ICAM1, VCAM1, E-selectin, and P-selectin, each of which enhances leukocyte-endothelium interactions and further promotes aggregation of macrophages in atherosclerotic lesions. The effects of Nkx2-5 on chemokines production were confusing, given that expression of C-X-C motif chemokine ligand 8 was inhibited and C-C motif chemokine ligand 5 augmented by Ad-Nkx2-5

infection. In addition, the local vascular renin-angiotensin system and angiogenesis may also be affected, given that we observed that angiotensin-converting enzyme (ACE) was inhibited and vascular endothelial growth factor (VEGF) A and C (VEGFA, VEGFC) upregulated.

Nkx2-5 Inhibits Monocyte-Endothelial Adhesion and Decreases Expression of Adhesion Molecules in Early Atherosclerosis

Given that compromised endothelial function is a hallmark of early atherosclerosis, the effects of Nkx2-5 on cell adhesion were further characterized. An endothelial cell monolayer adhesion assay was conducted, and we determined that pretreatment of cultured aortic endothelial cells with Ad-Nkx2-5 could significantly reduce the number of peripheral blood monocytes attached to TNFα-activated endothelial cell monolayers (Figure 8A and 8B). Simultaneously, expression of adhesion molecules ICAM1, VCAM1, E-selectin, and P-selectin were all decreased in endothelial cells, as evaluated by western blot and immunofluorescence assay (Figure 8A and 8C). In agreement with the above results, decreased expression of E-selectin and VCAM1 were also found in early atherosclerotic lesions of Ad-Nkx2-5-treated mice fed a chow diet, compared to their littermates treated with Ad-EV. Positive stained areas were quantified as a percentage of total plaque area or plaque endothelium (Figure 8D and 8E).

Given that it has been reported that NF-κB and MAPK signaling pathways play a critical role in mediating TNFα-induced endothelial cell activation, we investigated whether Nkx2-5 could suppress expression of adhesion molecules through inhibiting activation of these pathways. The three members of MAPK family, including c-Jun N-terminal kinase (JNK), extracellular signal-regulated kinase (ERK), and p38, were activated at 5 minutes after TNFα stimulation, as well as NF-κB pathway at 30 minutes (Figure S6A and S6C). However, Nkx2-5 overexpression had no effects on MAPK and NF-κB pathways in endothelial cells activated by TNFα or in the resting condition, as quantified by the relative phosphorylation of JNK, ERK, p38, inhibitor of NF-κB, and p65 (Figure S6B and S6D).

Furthermore, the 2200-bp promoter-luciferase reporter constructs of ICAM1, VCAM1, E-selectin, and P-selectin were established and transfected into HEK293 cells. Nkx2-5 overexpression significantly reduced the luciferase activity of all promoters except for VCAM1 (Figure S6E).

Discussion

This study provides novel evidence in the antiatherogenic effects of Nkx2-5, suggesting that Nkx2-5 is a physiological protector against vascular diseases.

Rupture-prone vulnerable plaques are susceptible to undergoing rapid progression and giving rise to superimposed thrombosis, ultimately leading to acute cardiovascular events. The vulnerable plaques are typically associated with the presence of highly inflammatory cell content and a large necrotic core covered by a thin, fibrous cap.[26] Moreover, increased elastolytic activity in the arterial wall also accelerates the progression and rupture of atherosclerotic plaques.[27] In contrast, the amount and organization of collagen and other matrix components is associated with the mechanical stability of the fibrous cap. In the present study, Nkx2-5 not only decreased lesion areas, but also induced a highly characteristic architecture of more-stable plaques, with decreased infiltrating macrophages, abundant collagen content, integral VSMC-rich fibrous caps overlying small necrotic cores, and a relatively well-preserved elastic lamina. It could be attributed, at least in part, to the regulation of Nkx2-5 on MMPs and TIMPs. Molecular studies revealed that Nkx2-5, as a key transcription factor, was recruited to the promoters of specific members of MMPs/TIMPs, thus directly regulated gene expression. As luciferase reporter gene assay demonstrated, Nkx2-5 overexpression significantly reduced the promoter activity of MMP2, MMP8, MMP9, MMP10, MMP11, and MMP14 and also enhanced TIMP1 promoter activity. For other MMPs/TIMPs that were not modified by Nkx2-5 in western blot assay (MMP1, MMP3, MMP7, TIMP3, and TIMP4), the promoter activities were unaffected by Nkx2-5 as expected. The regulation mechanism was further clarified in ChIP assay; Nkx2-5 enrichment in the specific binding sites of promoters was observed, including MMP2, MMP3, MMP8, MMP9, MMP10, MMP11, MMP14, and TIMP1. No significant occupancy of Nkx2-5 on the promoters of MMP1, MMP7, TIMP3, and TIMP4 was observed. Although some inconsistencies could not be ignored, the luciferase activities of MMP12, MMP13, and TIMP2 promoters were not affected by Nkx2-5, although western blot showed a significant increase in protein levels. This is probably because the promoter constructs, which range from −2000 to +200 bp, do not include the significant binding sites of Nkx2-5. Alternatively, the elevated protein levels of MMP12 and MMP13 might be attributed to compensatory reduced protein degradation, given that the majority of MMPs, including MMP2, MMP8, MMP9, MMP10, MMP11, and MMP14, were all repressed by Nkx2-5. Moreover, in ChIP assay, Nkx2-5 showed high enrichment in the MMP3 promoter, yet it might make little sense, given that western blot or dual luciferase reporter gene assay did not demonstrate any significant differences.

Given that the intriguing association between the expression/activity of specific MMPs and signs of plaque inflammation and matrix degradation was depicted in the early 1990s, an impressive effort has been made to precisely define the roles of MMPs in both the development and complications

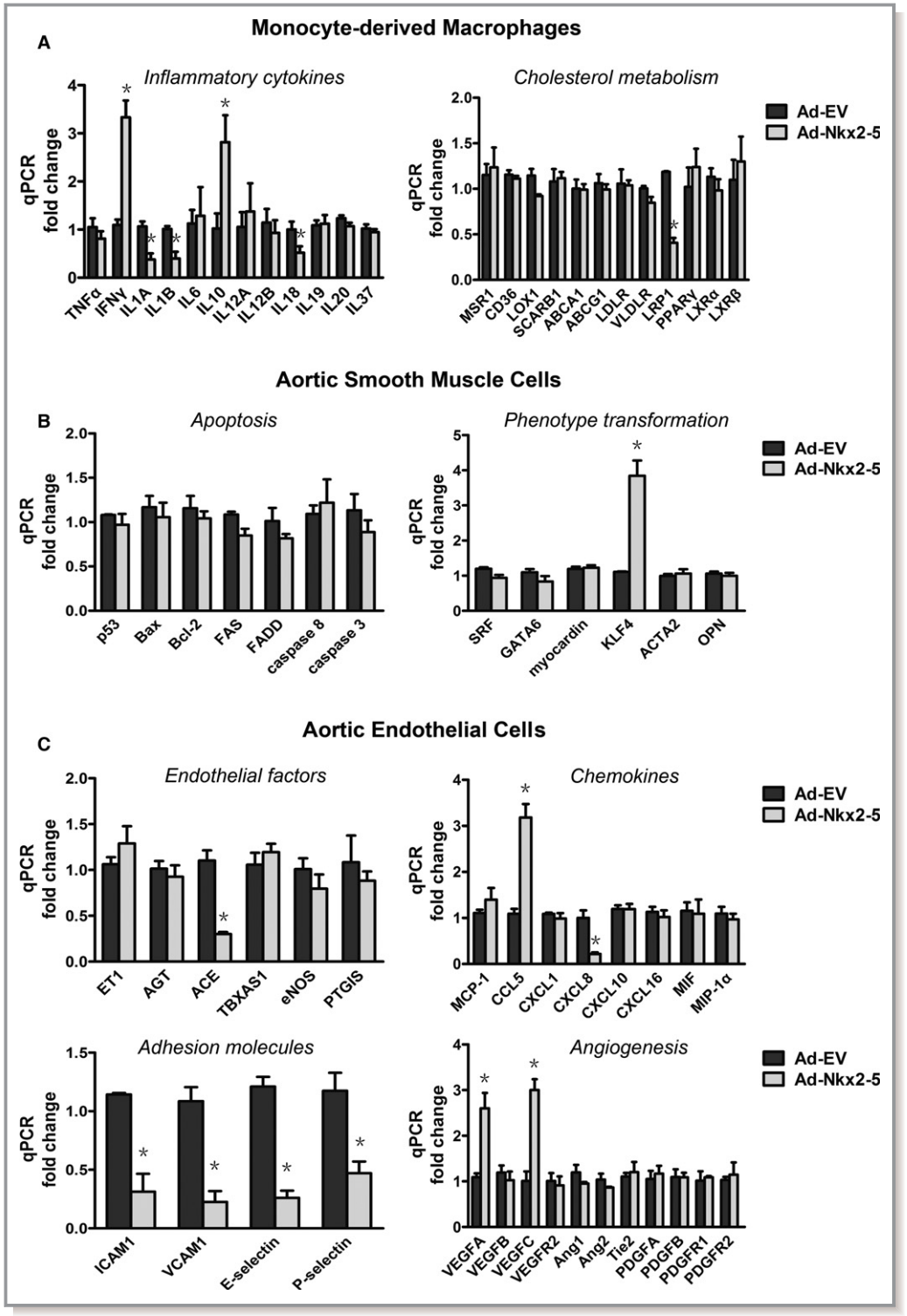

Figure 7. NK2 homeobox 5 (Nkx2-5) regulates the expression of extra functional genes in macrophages, smooth muscle cells, and endothelial cells. Cells treated with Ad-Nkx2-5 or Ad-EV for 24 hours were subjected to real-time polymerase chain reaction analysis. A, Relative mRNA expression levels of genes involved in inflammation and cholesterol metabolism of monocyte-derived macrophages. B, Relative mRNA expression levels of genes involved in apoptosis and phenotype transformation of aortic smooth muscle cells. C, Relative mRNA expression levels of endothelial factors involved in arterial vasomotoricity, chemokine production, adhesion, and angiogenesis. Data represent the mean±SEM of 3 independent experiments. *P<0.05 versus the Ad-EV-treated group. ICAM-1 indicates intercellular adhesion molecule-1; qPCR, quantitative polymerase chain reaction; VCAM-1, vascular cell adhesion molecule-1.

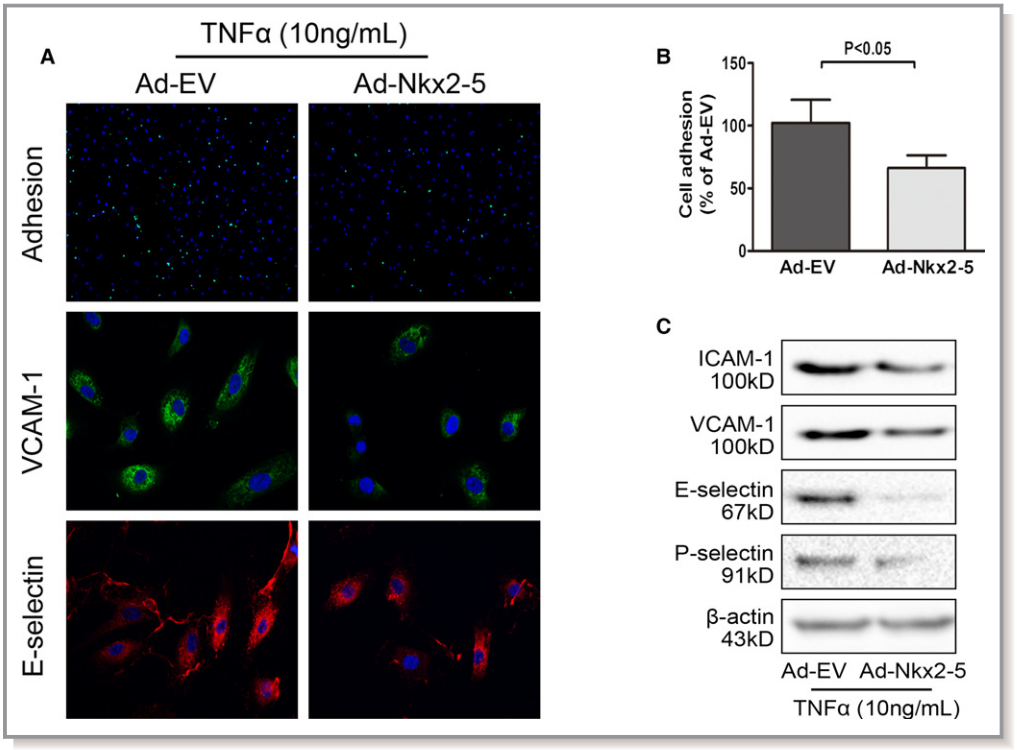

Figure 8. NK2 homeobox 5 (Nkx2-5) inhibits monocyte-endothelial adhesion and decreases expression of adhesion molecules in early atherosclerosis. A, Upper panel: representative images used for quantification of peripheral blood monocytes (PBMC; green, calcein AM) attached to aortic endothelial cells (HAECs, blue, DAPI). Middle panel: effects of Nkx2-5 on expression of vascular cell adhesion molecule-1 (VCAM-1) in endothelial cells (representative immunofluorescence image: green for VCAM-1 and blue for cell nuclei stained with DAPI). Lower panel: effects of Nkx2-5 on expression of E-selectin in endothelial cells (representative immunofluorescence image: red for E-selectin and blue for cell nuclei stained with DAPI). B, Quantification of adhesion. The number of PBMC adhered to per 100 HAECs was calculated. Results are expressed as a percent of values determined in the Ad-EV-treated group. Data represent the mean±SEM of 3 independent experiments. C, Representative immunoblot for intercellular adhesion molecule-1 (ICAM-1), VCAM-1, E-selectin, and P-selectin in endothelial cells infected with Ad-EV or Ad-Nkx2-5. D, Cross-sections of early atherosclerotic lesions in aortic sinus were immunostained with antibodies against von Willebrand factor (vWF), VCAM-1, and E-selectin. Staining with rabbit IgG isotype was used as the negative control. E, Quantification of histochemical staining of VCAM-1 and E-selectin. Positive stained areas were quantified as a percentage of total plaque area or plaque endothelium. Data are expressed as mean±SEM (n=12 per group). AM indicates acetomethoxy; DAPI, 4′,6-diamidino-2-phenylindole; HAECs, human aortic endothelial cells; IgG, immunoglobulin G; TNFα, tumor necrosis factor alpha.

of atherosclerosis.[28–30] Overexpression of MMP1 in macrophages resulted in smaller aortic atherosclerotic lesions with reduced fibrillar collagen content in ApoE$^{-/-}$ mice.[31] Lesion areas were significantly larger in ApoE$^{-/-}$MMP3$^{-/-}$ mice than in ApoE$^{-/-}$ mice.[32] In contrast, MMP7 may not make a major contribution to atherosclerotic plaque development or stability.[33] Mice lacking MMP13 accumulated more collagen with a more-organized supramolecular structure in plaques; so did MMP14 deficiency. MMP14 was also related to the activity regulation of other MMPs, such as MMP2 and MMP13.[34–37] Deficiency of MMP2, MMP8, or MMP9 led to smaller atherosclerotic lesions with fewer smooth muscle cells and reduced macrophage infiltration.[38–42] The roles of MMP12 in atherosclerosis are controversial and studies on MMP10 and MMP11 are still limited. Given that the majority of MMPs could be regulated by Nkx2-5, it was hard to determine which dominated in the progression of atherosclerosis and a comprehensive effect should be taken into consideration.

Compromised endothelial function is a hallmark of early atherosclerosis, and the leukocyte-endothelium interaction constitutes a key cellular event in the initiation of the disease.[43] Although we failed to detect Nkx2-5 expression in the endothelium of atherosclerotic plaques, Nkx2-5 gene transfer clearly ameliorated atherosclerosis at an early stage. It would be owing to the inhibitory effects on the expression of adhesion molecules such as E-selectin, P-selectin, ICAM1, and VCAM1. Activated NF-κB and MAPK pathways, which

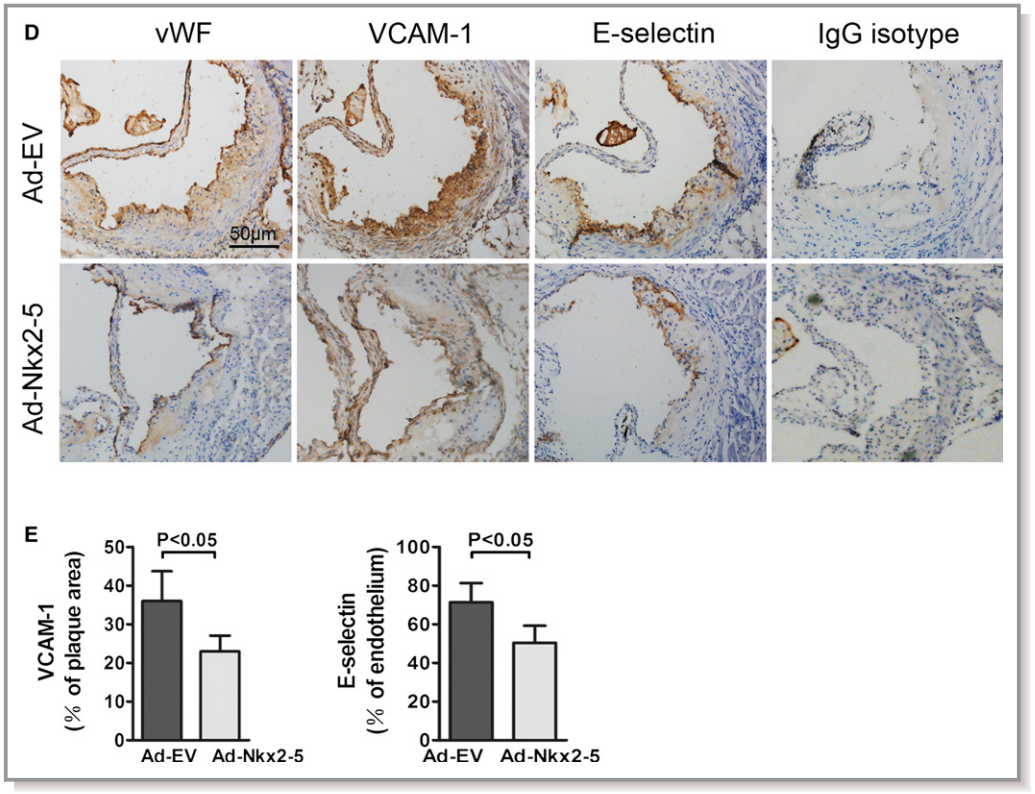

Figure 8. Continued

certainly augmented the expression of these adhesion molecules, could not be inhibited by Nkx2-5 either in resting conditions or in TNFα-activated cells. In contrast, the promoter luciferase activities of E-selectin, P-selectin, and ICAM1 were obviously suppressed by Nkx2-5. It indicated that these adhesion molecules, similar to MMPs and TIMPs, would most likely be the novel target genes of Nkx2-5. The luciferase activity of VCAM1 promoter was unaffected, probably because the key regulation region was not included in the construct, given that western blot and immunofluorescence in endothelial cells, as well as immunohistochemistry in atherosclerotic lesions, all demonstrated a significant decrease in VCAM1 protein level.

Besides involving in extracellular matrix remodeling and leukocyte-endothelium interaction, Nkx2-5 could exert more actions predicted to influence the progression of atherosclerosis, such as inflammatory response, phenotypic switching, and arterial vasomotoricity. Krüppel-like factor 4 (KLF4), which is not expressed in adult-differentiated smooth muscle cells, was upregulated by Nkx2-5 in vitro. Several studies provide evidence that KLF4 is re-expressed and involved in mediating smooth muscle cell phenotypic switching within lesions of ApoE$^{-/-}$ mice on a Western diet as well as following vascular injury.[44,45] Key questions include the following. Is Nkx2-5 involved in the increased expression of KLF4 in atherosclerotic lesions? Is KLF4-dependent smooth muscle cell phenotypic switching beneficial or detrimental? Considering a variety of target genes of Nkx2-5 involved in atherosclerosis, how much of a difference will KLF4 make? More research is needed to elaborate these questions. Nkx2-5 also exerted an inhibitory effect on ACE, a key enzyme of renin-angiotensin-aldosterone system (RAAS). Accumulating evidence suggests that inappropriate activation of local tissue RAAS in vascular tissue, immune cells, and perivascular adipose tissue is associated with endothelial dysfunction and arterial stiffness.[46–48] However, a conclusion could not be reached simply because the activity of this enzyme has not been determinated. This holds for some other critical enzymes, such as endothelia nitric oxide (NO) synthase, thromboxane A synthase 1, and prostaglandin I2 synthase. Further analysis of enzyme activities will help us clarify the exact role of Nkx2-5 in the endothelial functions. Moreover, upregulation of VEGFA and VEGFC in Ad-Nkx2-5-treated endothelial cells seemed inconsistent with our previous conclusion, given that VEGF induces endothelial cell proliferation, promotes cell migration, and increases cell adhesion.[49–51] However, the effects of VEGF may not predominate given that leukocyte-endothelial cell adhesion was obviously inhibited by Nkx2-5. There are reasons to think that these effects were attributed to the direct inhibition of Nkx2-5 on major adhesion molecules. Furthermore, roles of VEGF in vascular biology remain highly

controversial. Both systemic and local VEGF gene transfer protected from neointimal growth, a phenomenon that has been reported to be, in part, NO dependent.[52–54] Concomitantly, systemic VEGF inhibition accelerates experimental atherosclerosis and disrupts endothelial homeostasis.[55] A single intraperitoneal application of VEGF, however, did increase atherosclerosis in different animal models.[56] The opposing effects of VEGF appear to markedly depend on local VEGF concentrations, stage of the disease, and different experimental conditions. Although these additional functions were just preliminarily validated in cultured cells, we have reason to believe that the effects of Nkx2-5 on atherosclerosis are comprehensive, involving multiple kinds of cells and different pathological processes.

In the present study, intraventricular adenovirus gene transfer was used to manipulate Nkx2-5 expression in aorta, and exposure of mice to a Western diet before adenovirus administration reflected the situation of elderly patients with pre-existing atherosclerosis. However, whether the antiatherogenic effects of Nkx2-5 were partially mediated by cross-talk between arteries and remote organs remained elusive, given that systemic adenovirus gene transfer actually affected various tissues and dynamic multiple organ cross-talk in atherosclerosis has been paid much emphasis.[57,58] To further elucidate the effects of Nkx2-5 on specific cell types of certain tissues, cell-type–selective genetic manipulation should be taken into account in our future studies.

Taken together, our present study suggests that Nkx2-5 could ameliorate and stabilize the advanced atherosclerotic plaques, which may partly be attributed to the regulation on MMPs and TIMPs in macrophages and smooth muscle cells. As well, Nkx2-5 significantly represses expression of adhesion molecules in endothelial cells and therefore improves endothelium functions and inhibits progression of atherosclerosis at an early stage.

Sources of Funding

This work was supported by the National Natural Science Foundation of China (30971245 to Kai Huang and 81000112 to Dan Huang).

Disclosures

None.

References

1. Prall OW, Menon MK, Solloway MJ, Watanabe Y, Zaffran S, Bajolle F, Biben C, McBride JJ, Robertson BR, Chaulet H, Stennard FA, Wise N, Schaft D, Wolstein O, Furtado MB, Shiratori H, Chien KR, Hamada H, Black BL, Saga Y, Robertson EJ, Buckingham ME, Harvey RP. An Nkx2-5/Bmp2/Smad1 negative feedback loop controls heart progenitor specification and proliferation. *Cell*. 2007;128:947–959.
2. Komuro I, Izumo S. Csx: a murine homeobox-containing gene specifically expressed in the developing heart. *Proc Natl Acad Sci USA*. 1993;90:8145–8149.
3. Lints TJ, Parsons LM, Hartley L, Lyons I, Harvey RP. Nkx-2.5: a novel murine homeobox gene expressed in early heart progenitor cells and their myogenic descendants. *Development*. 1993;119:419–431.
4. Lyons I, Parsons LM, Hartley L, Li R, Andrews JE, Robb L, Harvey RP. Myogenic and morphogenetic defects in the heart tubes of murine embryos lacking the homeo box gene Nkx2-5. *Genes Dev*. 1995;9:1654–1666.
5. Tanaka M, Chen Z, Bartunkova S, Yamasaki N, Izumo S. The cardiac homeobox gene Csx/Nkx2.5 lies genetically upstream of multiple genes essential for heart development. *Development*. 1999;126:1269–1280.
6. Wu SM, Fujiwara Y, Cibulsky SM, Clapham DE, Lien CL, Schultheiss TM, Orkin SH. Developmental origin of a bipotential myocardial and smooth muscle cell precursor in the mammalian heart. *Cell*. 2006;127:1137–1150.
7. Nakano H, Liu X, Arshi A, Nakashima Y, van Handel B, Sasidharan R, Harmon AW, Shin JH, Schwartz RJ, Conway SJ, Harvey RP, Pashmforoush M, Mikkola HK, Nakano A. Haemogenic endocardium contributes to transient definitive haematopoiesis. *Nat Commun*. 2013;4:1564.
8. Benson DW, Silberbach GM, Kavanaugh-McHugh A, Cottrill C, Zhang Y, Riggs S, Smalls O, Johnson MC, Watson MS, Seidman JG, Seidman CE, Plowden J, Kugler JD. Mutations in the cardiac transcription factor NKX2.5 affect diverse cardiac developmental pathways. *J Clin Invest*. 1999;104:1567–1573.
9. Elliott DA, Kirk EP, Yeoh T, Chandar S, McKenzie F, Taylor P, Grossfeld P, Fatkin D, Jones O, Hayes P, Feneley M, Harvey RP. Cardiac homeobox gene NKX2-5 mutations and congenital heart disease: associations with atrial septal defect and hypoplastic left heart syndrome. *J Am Coll Cardiol*. 2003;41:2072–2076.
10. McElhinney DB, Geiger E, Blinder J, Benson DW, Goldmuntz E. NKX2.5 mutations in patients with congenital heart disease. *J Am Coll Cardiol*. 2003;42:1650–1655.
11. Schott JJ, Benson DW, Basson CT, Pease W, Silberbach GM, Moak JP, Maron BJ, Seidman CE, Seidman JG. Congenital heart disease caused by mutations in the transcription factor NKX2-5. *Science*. 1998;281:108–111.
12. Habets PE, Moorman AF, Clout DE, van Roon MA, Lingbeek M, van Lohuizen M, Campione M, Christoffels VM. Cooperative action of Tbx2 and Nkx2.5 inhibits ANF expression in the atrioventricular canal: implications for cardiac chamber formation. *Genes Dev*. 2002;16:1234–1246.
13. Jay PY, Harris BS, Maguire CT, Buerger A, Wakimoto H, Tanaka M, Kupershmidt S, Roden DM, Schultheiss TM, O'Brien TX, Gourdie RG, Berul CI, Izumo S. Nkx2-5 mutation causes anatomic hypoplasia of the cardiac conduction system. *J Clin Invest*. 2004;113:1130–1137.
14. Pashmforoush M, Lu JT, Chen H, Amand TS, Kondo R, Pradervand S, Evans SM, Clark B, Feramisco JR, Giles W, Ho SY, Benson DW, Silberbach M, Shou W, Chien KR. Nkx2-5 pathways and congenital heart disease; loss of ventricular myocyte lineage specification leads to progressive cardiomyopathy and complete heart block. *Cell*. 2004;117:373–386.
15. Rivers ER, Horton AJ, Hawk AF, Favre EG, Senf KM, Nietert PJ, Chang EY, Foley AC, Robinson CJ, Lee KH. Placental Nkx2-5 and target gene expression in early-onset and severe preeclampsia. *Hypertens Pregnancy*. 2014;33:412–426.
16. van Engelen K, Mommersteeg MT, Baars MJ, Lam J, Ilgun A, van Trotsenburg AS, Smets AM, Christoffels VM, Mulder BJ, Postma AV. The ambiguous role of NKX2-5 mutations in thyroid dysgenesis. *PLoS One*. 2012;7:e52685.
17. Hwang C, Jang S, Choi DK, Kim S, Lee JH, Lee Y, Kim CD. The role of nkx2.5 in keratinocyte differentiation. *Ann Dermatol*. 2009;21:376–381.
18. Nagel S, Scherr M, Kel A, Hornischer K, Crawford GE, Kaufmann M, Meyer C, Drexler HG, MacLeod RA. Activation of TLX3 and NKX2-5 in t(5;14)(q35;q32) T-cell acute lymphoblastic leukemia by remote 3′-BCL11B enhancers and coregulation by PU.1 and HMGA1. *Cancer Res*. 2007;67:1461–1471.
19. Przybylski GK, Dik WA, Grabarczyk P, Wanzeck J, Chudobska P, Jankowski K, von Bergh A, van Dongen JJ, Schmidt CA, Langerak AW. The effect of a novel recombination between the homeobox gene NKX2-5 and the TRD locus in t-cell acute lymphoblastic leukemia on activation of the NKX2-5 gene. *Haematologica*. 2006;91:317–321.
20. Nagel S, Kaufmann M, Drexler HG, MacLeod RA. The cardiac homeobox gene NKX2-5 is deregulated by juxtaposition with BCL11B in pediatric T-ALL cell lines via a novel t(5;14)(q35.1;q32.2). *Cancer Res*. 2003;63:5329–5334.
21. Tian Y, Sommerville LJ, Cuneo A, Kelemen SE, Autieri MV. Expression and suppressive effects of interleukin-19 on vascular smooth muscle cell pathophysiology and development of intimal hyperplasia. *Am J Pathol*. 2008;173:901–909.
22. Cuneo AA, Herrick D, Autieri MV. IL-19 reduces VSMC activation by regulation of mRNA regulatory factor HuR and reduction of mRNA stability. *J Mol Cell Cardiol*. 2010;49:647–654.

23. Sommerville LJ, Kelemen SE, Ellison SP, England RN, Autieri MV. Increased atherosclerosis and vascular smooth muscle cell activation in AIF-1 transgenic mice fed a high-fat diet. *Atherosclerosis*. 2012;220:45–52.
24. Oh LY, Larsen PH, Krekoski CA, Edwards DR, Donovan F, Werb Z, Yong VW. Matrix metalloproteinase-9/gelatinase B is required for process outgrowth by oligodendrocytes. *J Neurosci*. 1999;19:8464–8475.
25. Wang X, Liang J, Koike T, Sun H, Ichikawa T, Kitajima S, Morimoto M, Shikama H, Watanabe T, Sasaguri Y, Fan J. Overexpression of human matrix metalloproteinase-12 enhances the development of inflammatory arthritis in transgenic rabbits. *Am J Pathol*. 2004;165:1375–1383.
26. Silvestre-Roig C, de Winther MP, Weber C, Daemen MJ, Lutgens E, Soehnlein O. Atherosclerotic plaque destabilization: mechanisms, models, and therapeutic strategies. *Circ Res*. 2014;114:214–226.
27. Watanabe N, Ikeda U. Matrix metalloproteinases and atherosclerosis. *Curr Atheroscler Rep*. 2004;6:112–120.
28. Henney AM, Wakeley PR, Davies MJ, Foster K, Hembry R, Murphy G, Humphries S. Localization of stromelysin gene expression in atherosclerotic plaques by in situ hybridization. *Proc Natl Acad Sci USA*. 1991;88:8154–8158.
29. Galis ZS, Sukhova GK, Lark MW, Libby P. Increased expression of matrix metalloproteinases and matrix degrading activity in vulnerable regions of human atherosclerotic plaques. *J Clin Invest*. 1994;94:2493–2503.
30. Galis ZS, Sukhova GK, Kranzhofer R, Clark S, Libby P. Macrophage foam cells from experimental atheroma constitutively produce matrix-degrading proteinases. *Proc Natl Acad Sci USA*. 1995;92:402–406.
31. Lemaitre V, O'Byrne TK, Borczuk AC, Okada Y, Tall AR, D'Armiento J. ApoE knockout mice expressing human matrix metalloproteinase-1 in macrophages have less advanced atherosclerosis. *J Clin Invest*. 2001;107:1227–1234.
32. Silence J, Lupu F, Collen D, Lijnen HR. Persistence of atherosclerotic plaque but reduced aneurysm formation in mice with stromelysin-1 (MMP-3) gene inactivation. *Arterioscler Thromb Vasc Biol*. 2001;21:1440–1445.
33. Johnson JL, George SJ, Newby AC, Jackson CL. Divergent effects of matrix metalloproteinases 3, 7, 9, and 12 on atherosclerotic plaque stability in mouse brachiocephalic arteries. *Proc Natl Acad Sci USA*. 2005;102:15575–15580.
34. Deguchi JO, Aikawa E, Libby P, Vachon JR, Inada M, Krane SM, Whittaker P, Aikawa M. Matrix metalloproteinase-13/collagenase-3 deletion promotes collagen accumulation and organization in mouse atherosclerotic plaques. *Circulation*. 2005;112:2708–2715.
35. Schneider F, Sukhova GK, Aikawa M, Canner J, Gerdes N, Tang SM, Shi GP, Apte SS, Libby P. Matrix-metalloproteinase-14 deficiency in bone-marrow-derived cells promotes collagen accumulation in mouse atherosclerotic plaques. *Circulation*. 2008;117:931–939.
36. Visse R, Nagase H. Matrix metalloproteinases and tissue inhibitors of metalloproteinases: structure, function, and biochemistry. *Circ Res*. 2003;92:827–839.
37. Egeblad M, Werb Z. New functions for the matrix metalloproteinases in cancer progression. *Nat Rev Cancer*. 2002;2:161–174.
38. Kuzuya M, Nakamura K, Sasaki T, Cheng XW, Itohara S, Iguchi A. Effect of MMP-2 deficiency on atherosclerotic lesion formation in apoE-deficient mice. *Arterioscler Thromb Vasc Biol*. 2006;26:1120–1125.
39. Galis ZS, Johnson C, Godin D, Magid R, Shipley JM, Senior RM, Ivan E. Targeted disruption of the matrix metalloproteinase-9 gene impairs smooth muscle cell migration and geometrical arterial remodeling. *Circ Res*. 2002;91:852–859.
40. Luttun A, Lutgens E, Manderveld A, Maris K, Collen D, Carmeliet P, Moons L. Loss of matrix metalloproteinase-9 or matrix metalloproteinase-12 protects apolipoprotein E-deficient mice against atherosclerotic media destruction but differentially affects plaque growth. *Circulation*. 2004;109:1408–1414.
41. Johnson C, Galis ZS. Matrix metalloproteinase-2 and -9 differentially regulate smooth muscle cell migration and cell-mediated collagen organization. *Arterioscler Thromb Vasc Biol*. 2004;24:54–60.
42. Lenglet S, Mach F, Montecucco F. Role of matrix metalloproteinase-8 in atherosclerosis. *Mediators Inflamm*. 2013;2013:659282.
43. Galkina E, Ley K. Vascular adhesion molecules in atherosclerosis. *Arterioscler Thromb Vasc Biol*. 2007;27:2292–2301.
44. Cherepanova OA, Pidkovka NA, Sarmento OF, Yoshida T, Gan Q, Adiguzel E, Bendeck MP, Berliner J, Leitinger N, Owens GK. Oxidized phospholipids induce type VIII collagen expression and vascular smooth muscle cell migration. *Circ Res*. 2009;104:609–618.
45. Yoshida T, Kaestner KH, Owens GK. Conditional deletion of Kruppel-like factor 4 delays downregulation of smooth muscle cell differentiation markers but accelerates neointimal formation following vascular injury. *Circ Res*. 2008;102:1548–1557.
46. Brillante DG, O'Sullivan AJ, Howes LG. Arterial stiffness in insulin resistance: the role of nitric oxide and angiotensin II receptors. *Vasc Health Risk Manag*. 2009;5:73–78.
47. Nyby MD, Abedi K, Smutko V, Eslami P, Tuck ML. Vascular angiotensin type 1 receptor expression is associated with vascular dysfunction, oxidative stress and inflammation in fructose-fed rats. *Hypertens Res*. 2007;30:451–457.
48. Shinozaki K, Ayajiki K, Nishio Y, Sugaya T, Kashiwagi A, Okamura T. Evidence for a causal role of the renin-angiotensin system in vascular dysfunction associated with insulin resistance. *Hypertension*. 2004;43:255–262.
49. Soga N, Connolly JO, Chellaiah M, Kawamura J, Hruska KA. Rac regulates vascular endothelial growth factor stimulated motility. *Cell Commun Adhes*. 2001;8:1–13.
50. Wang Y, Zang QS, Liu Z, Wu Q, Maass D, Dulan G, Shaul PW, Melito L, Frantz DE, Kilgore JA, Williams NS, Terada LS, Nwariaku FE. Regulation of VEGF-induced endothelial cell migration by mitochondrial reactive oxygen species. *Am J Physiol Cell Physiol*. 2011;301:C695–C704.
51. Neufeld G, Cohen T, Gengrinovitch S, Poltorak Z. Vascular endothelial growth factor (VEGF) and its receptors. *FASEB J*. 1999;13:9–22.
52. Hiltunen MO, Laitinen M, Turunen MP, Jeltsch M, Hartikainen J, Rissanen TT, Laukkanen J, Niemi M, Kossila M, Hakkinen TP, Kivela A, Enholm B, Mansukoski H, Turunen AM, Alitalo K, Yla-Herttuala S. Intravascular adenovirus-mediated VEGF-C gene transfer reduces neointima formation in balloon-denuded rabbit aorta. *Circulation*. 2000;102:2262–2268.
53. Laitinen M, Zachary I, Breier G, Pakkanen T, Hakkinen T, Luoma J, Abedi H, Risau W, Soma M, Laakso M, Martin JF, Yla-Herttuala S. VEGF gene transfer reduces intimal thickening via increased production of nitric oxide in carotid arteries. *Hum Gene Ther*. 1997;8:1737–1744.
54. Asahara T, Bauters C, Pastore C, Kearney M, Rossow S, Bunting S, Ferrara N, Symes JF, Isner JM. Local delivery of vascular endothelial growth factor accelerates reendothelialization and attenuates intimal hyperplasia in balloon-injured rat carotid artery. *Circulation*. 1995;91:2793–2801.
55. Winnik S, Lohmann C, Siciliani G, von Lukowicz T, Kuschnerus K, Kraenkel N, Brokopp CE, Enseleit F, Michels S, Ruschitzka F, Luscher TF, Matter CM. Systemic VEGF inhibition accelerates experimental atherosclerosis and disrupts endothelial homeostasis–implications for cardiovascular safety. *Int J Cardiol*. 2013;168:2453–2461.
56. Celletti FL, Waugh JM, Amabile PG, Brendolan A, Hilfiker PR, Dake MD. Vascular endothelial growth factor enhances atherosclerotic plaque progression. *Nat Med*. 2001;7:425–429.
57. Swirski FK, Nahrendorf M, Etzrodt M, Wildgruber M, Cortez-Retamozo V, Panizzi P, Figueiredo JL, Kohler RH, Chudnovskiy A, Waterman P, Aikawa E, Mempel TR, Libby P, Weissleder R, Pittet MJ. Identification of splenic reservoir monocytes and their deployment to inflammatory sites. *Science*. 2009;325:612–616.
58. Das R, Ganapathy S, Mahabeleshwar GH, Drumm C, Febbraio M, Jain MK, Plow EF. Macrophage gene expression and foam cell formation are regulated by plasminogen. *Circulation*. 2013;127:1209–1218, e1201-1216.

SUPPLEMENTAL MATERIAL

Table S1. qRT-PCR primers used

Gene	Forward primer	Reverse primer
TNFα	CCCAGGGACCTCTCTCTAATC	ATGGGCTACAGGCTTGTCACT
IFNγ	TCGGTAACTGACTTGAATGTCCA	TCGCTTCCCTGTTTTAGCTGC
IL1A	TGGTAGTAGCAACCAACGGGA	ACTTTGATTGAGGGCGTCATTC
IL1B	TTCGACACATGGGATAACGAGG	TTTTTGCTGTGAGTCCCGGAG
IL6	ACTCACCTCTTCAGAACGAATTG	CCATCTTTGGAAGGTTCAGGTTG
IL10	GACTTTAAGGGTTACCTGGGTTG	TCACATGCGCCTTGATGTCTG
IL12A	ATGGCCCTGTGCCTTAGTAGT	AGCTTTGCATTCATGGTCTTGA
IL12B	ACCCTGACCATCCAAGTCAAA	TTGGCCTCGCATCTTAGAAAG
IL18	TCTTCATTGACCAAGGAAATCGG	TCCGGGGTGCATTATCTCTAC
IL19	ATCCAAGCTAAGGACACCTTCC	GTCACGCAGCACACATCTAAG
IL20	ATGAAAGCCTCTAGTCTTGCCT	GCCCCGTATCTCAGAAAATCC
IL37	TTCTTTGCATTAGCCTCATCCTT	CGTGCTGATTCCTTTTGGGC
MSR1	GCAGTGGGATCACTTTCACAA	AGCTGTCATTGAGCGAGCATC
CD36	GGCTGTGACCGGAACTGTG	AGGTCTCCAACTGGCATTAGAA
LOX1	AATGATAGAAACCCTTGC	TTCCCAGTTAAATGAGCC
SCARB1	AATAAGCCCATGACCCTGAAGC	GCCCCACATGATCTCACCC
ABCA1	ACCCACCCTATGAACAACATGA	GAGTCGGGTAACGGAAACAGG
ABCG1	ATTCAGGGACCTTTCCTATTCGG	CTCACCACTATTGAACTTCCCG
LDLR	ACGGCGTCTCTTCCTATGACA	CCCTTGGTATCCGCAACAGA
VLDLR	AGAAAAGCCAAATGTGAACCCT	CACTGCCGTCAACACAGTCT

LRP1	CTTCAAGAACGCAGTGGTG	CAGTAGAGTTTGCTTTCAGGGA
PPARγ	ACCAAAGTGCAATCAAAGTGGA	ATGAGGGAGTTGGAAGGCTCT
LXRα	CCTTCAGAACCCACAGAGATCC	ACGCTGCATAGCTCGTTCC
LXRβ	AGAAGATTCGGAAACAACAGCA	GCTGGATCATTAGTTCTTGAGCC
p53	CCACCATCCACTACAACTACAT	AGGACAGGCACAAACACG
Bax	TCTGACGGCAACTTCAACTG	AGGAAAACGCATTATAGACCAC
Bcl-2	CTGGGAGAACAGGGTACGATAA	GGCTGGGAGGAGAAGATGC
FAS	GATGGCCAATTCTGCCATAAG	GTCTGGTTCATCCCCATTGACT
FADD	GTGGCTGACCTGGTACAAGAG	GGTAGATGCGTCTGAGTTCCAT
caspase 3	CATGGAAGCGAATCAATGGACT	CTGTACCAGACCGAGATGTCA
caspase 8	GTTGTGTGGGGTAATGACAATCT	TCAAAGGTCGTGGTCAAAGCC
SRF	CCGGCAAGGCACTGATTCA	CTCATTCTCTGGTCTGTTGTGG
GATA6	CTCAGTTCCTACGCTTCGCAT	GTCGAGGTCAGTGAACAGCA
myocardin	CCACCTATGGACTCAGCCTAC	CTCAGTGGCGTTGAAGAAGAG
KLF4	CCCACATGAAGCGACTTCCC	CAGGTCCAGGAGATCGTTGAA
ACTA2	AAAAGACAGCTACGTGGGTGA	GCCATGTTCTATCGGGTACTTC
OPN	GAAGTTTCGCAGACCTGACAT	GTATGCACCATTCAACTCCTCG
ET1	AGAGTGTGTCTACTTCTGCCA	CTTCCAAGTCCATACGGAACAA
AGT	CCCCAGTCTGAGATGGCTC	GACGAGGTGGAAGGGGTGTA
ACE	GGAGGAATATGACCGGACATCC	TGGTTGGCTATTTGCATGTTCTT
TBXAS1	GTATGGACCTCTGTGTGGGTA	CCGACGCCATTCTGTTGGTAA
eNOS	TGATGGCGAAGCGAGTGAAG	ACTCATCCATACACAGGACCC

PTGIS	CTGTTGGGCGATGCTACAGAA	GCCTCAATTCCGTAAAGAGTCA
MCP-1	CTTCTGTGCCTGCTGCTCAT	CGGAGTTTGGGTTTGCTTGTC
CCL5	CCAGCAGTCGTCTTTGTCAC	CTCTGGGTTGGCACACACTT
CXCL1	CCCCAAGAACATCCAAAGTG	GATGCAGGATTGAGGCAAG
CXCL8	GTCCTTGTTCCACTGTGCCT	GCTTCCACATGTCCTCACAA
CXCL10	GTGGCATTCAAGGAGTACCTC	TGATGGCCTTCGATTCTGGATT
CXCL16	CCCGCCATCGGTTCAGTTC	CCCCGAGTAAGCATGTCCAC
MIF	GAACCGCTCCTACAGCAAGCT	GCGAAGGTGGAGTTGTTCCA
MIP-1α	AGTTCTCTGCATCACTTGCTG	CGGCTTCGCTTGGTTAGGAA
ICAM1	TTGGGCATAGAGACCCCGTT	GCACATTGCTCAGTTCATACACC
VCAM1	GGGAAGATGGTCGTGATCCTT	TCTGGGGTGGTCTCGATTTTA
E-selectin	GCACAGCCTTGTCCAACC	ACCTCACCAAACCCTTCG
P-selectin	ATGGGTGGGAACCAAAAAGG	GGCTGACGGACTCTTGATGTAT
VEGFA	AGGGCAGAATCATCACGAAGT	AGGGTCTCGATTGGATGGCA
VEGFB	GAGATGTCCCTGGAAGAACACA	GAGTGGGATGGGTGATGTCAG
VEGFC	GAGGAGCAGTTACGGTCTGTG	TCCTTTCCTTAGCTGACACTTGT
VEGFR2	GGCCCAATAATCAGAGTGGCA	CCAGTGTCATTTCCGATCACTTT
Ang1	AGCGCCGAAGTCCAGAAAAC	TACTCTCACGACAGTTGCCAT
Ang2	CTCGAATACGATGACTCGGTG	TCATTAGCCACTGAGTGTTGTTT
Tie2	TTAGCCAGCTTAGTTCTCTGTGG	AGCATCAGATACAAGAGGTAGGG
PDGFA	GCAAGACCAGGACGGTCATTT	GGCACTTGACACTGCTCGT
PDGFB	CTCGATCCGCTCCTTTGATGA	CGTTGGTGCGGTCTATGAG

PDGFR1	TTTTTGTGACGGTCTTGGAAGT	TGTCTGAGTGTGGTTGTAATAGC
PDGFR2	TGATGCCGAGGAACTATTCATCT	TTTCTTCTCGTGCAGTGTCAC

Table S2. Primers designed for promoter reporter gene construction

Gene	Primers	Promoter region (bp)	Promoter length (bp)
MMP1	**F** ATCTGCCACTCCTTGACT	-1784 ～ -466	1319
	R GCTTCCCTTAATCTTTACTC		
MMP2	**F** CAAGACATAATCGTGACCTCCAAT	-1556 ～ +55	1611
	R ACCGCCTGAGGAAGTCTGGAT		
MMP3	**F** TATTATCTATCAGGCTTTCC	-1870 ～ +66	1936
	R TTTCCACTGGCTTTACTT		
MMP7	**F** TAGGATTACAGGCGTGAG	-1601 ～ +22	1623
	R TTGGACCTATGGTTGATTTG		
MMP8	**F** TACTCTAGCACCCATCAC	-1399 ～ +69	1468
	R CTTTCTTTCTGTCCCTCT		
MMP9	**F** GCCCAAGGTCACATAGCT	-1932 ～ +199	2051
	R CTCCAGGGAAGAGCACAA		
MMP10	**F** ATGGCAGCACAGTAGGTT	-1936 ～ -214	1723
	R ATTGGCTAGATAATTCACGT		
MMP11	**F** AGGCCCTTCATCATTTCAG	-1538 ～ -185	1354
	R GGCAAAGTCCCTATCTGGT		
MMP12	**F** AATGGAGTAGCCTGTAAT	-1812 ～ +58	1870
	R CTTTCTAGCCTAAGTTCC		
MMP13	**F** CTCTAAGGCACTGGCTAC	-1616 ～ +170	1776

	R AGGATTGGCAAGATACTC		
MMP14	**F** TAGGCCATGTACAGCTGGCATC	-1541 ~ +162	1703
	R ACCGCTGTCGGCTTGGAGTT		
TIMP1	**F** TCACCCGAGGTCAGGAGT	-1882 ~ +10	1892
	R GCCGACGAAAGGAGATACAC		
TIMP2	**F** CGCCTCTCGGGTTCAAGCGA	-1559 ~ +30	1589
	R CGCGCTGCCTTCTACGGATG		
TIMP3	**F** TATTAGGCTCATGGACACC	-1744 ~ -68	1677
	R AGAAAGGCAAGAGGAAGT		
TIMP4	**F** CTACACTGAGGTAGCCATAC	-1541 ~ +183	1724
	R GAAAGAGCCACAAAGACA		
ICAM1	**F** CTGCCCTGTCATCTCCCT	-1753 ~ -86	1668
	R TCCATTTCACAAAGCGGTA		
VCAM1	**F** CTGGGAGGAGCAGGTAGGA	-1718 ~ +66	1784
	R TTGTTGCAGAGGCGGAGG		
E-selectin	**F** TTTGGGTCTTGACATCTT	-1903 ~ +67	1970
	R GGTATCACTGCTGCCTCT		
P-selectin	**F** AGCGTGATAGGTATTGTT	-1822 ~ +61	1883
	R TCTGTGACTCTGCTGGTT		

Table S3. Specific primers used in Chromatin immunoprecipitation Assay

Gene	Putative binding site of Nkx2-5	Primers	Product length (bp)
MMP1	**seq1** GGGCTCAAGTGATTCCCCT (-559 ～ -541)	**F** ACCTCAGCCTCTTCAGTG **R** GCTCAAGCCTATAATCCC	194
	seq2 TAAAGTGAGTGCTGGGGGA (-387 ～ -369)	**F** GGCAGCTTAACAAAGGCAGAA **R** CAGGGCAGAGGGTGGAAT	144
MMP2	**seq1** AGACATAATCGTGACCTCC (-1555 ～ -1536)	**F** CTGAAGCCCACTGAGACC **R** GCAGGGAACAGTTTGAGAA	141
	seq2 AAGAGTGAGTGGGGAATTC (-1015 ～ -999)	**F** GCTGAAGTCAGGCGTTCC **R** AGCCCTCAGTTCCACGAA	214
MMP3	**seq1** AGGAGAATCACTTGAGCCC (-1499 ～ -1481)	**F** CTGCCACCACTCTGTTCT **R** TGGGCTCAAGTGATTCTCC	211
	seq2 TCCAATGTTTATTAAGAAA (-1264 ～ -1246)	**F** TCTTCAGTCATAGGGATC **R** AGACCTTTAATAAGTGCC	162
	seq3 TGTTCAGGTAATTAACACT (+164～ +182)	**F** AGACAACATAGAGCTAAG **R** CCACCTGGCCAGGTCAGT	168
MMP7	**seq1** TGCTCATTCACTTGAGGAA (-1523 ～ -1505)	**F** TTTCCCAGGCTTGTCTCA **R** TTTTGGTAATATTTGCAT	200
	seq2 AAAGAAAACACTCAAATGA (-83 ～ -65)	**F** CTGCCAATAACGATGTAA **R** CTTCTCAGCCTCGAATGT	132

	seq3 AGGCATGAGTGAGCTACAG	**F** AGCTATGCGACTCACCGTG	157
	(+122～ +140)	**R** AGATGGCAAAAGAATGGAA	
MMP8	**seq1** AGACTCAAGTGGGAGACTA	**F** CCTTGTCTTCTGCCTGTG	187
	(-825 ～ -807)	**R** TGTTTCATTTGTGGAGGG	
	seq2 AATCATAATTTTTTAGCAA	**F** ACAAATGTCTGGGCAATC	145
	(-583 ～ -565)	**R** CTTCTGGAGGATGTGGTT	
	seq3 TAAGTTAATTCAACCTCAA	**F** CCACATACAATGAGGGAG	172
	(-303 ～ -285)	**R** AAAGGAACAAGGGACTAA	
	seq4 AGCTGTGAGTGACACATGA	**F** CCTATGTTGCTTCATATT	204
	(-10 ～ +9)	**R** GAAATGGAAGCGTCTTCAGG	
MMP9	**seq1** GAAGTTAATTATCTCCATC	**F** AATCCAGGACTTCGTGAC	151
	(-1617 ～ -1598)	**R** TAAAGGGCCTACTATGTG	
	seq2 GGGCAGATCACTTGAGTCA	**F** CCCGTAATCCTAGCACTT	257
	(-1474 ～ -1455)	**R** TGTAGTATCACTCTGTCACCC	
	seq3 TGTGATAATTGGGGCTGGA	**F** TTTCCCAGGCTTGTCTCA	201
	(-1072 ～ -1053)	**R** TTTTGGTAATATTTGCAT	
MMP10	**seq1** ATTATCAAGAATTATGTAC	**F** AGTCATTTATCACTATTAT	231
	(-1985 ～ -1967)	**R** AAGTTACCCAGTCTCAGG	
	seq2 GAACATAATTATACACTGG	**F** AGCAAAGAAGAGGAAGAGGGTA	209
	(-613 ～ -595)	**R** TACTGGCCGTGGAGTAGGG	
	seq3 CTACTTAATTCTTACCTGC	**F** CCACATTTAGACCACGAC	65
	(-365 ～ -347)	**R** AAGCAGGTAAGAATTAAGTAGG	

	seq4 TCCTCTGAGTGGGGCAGCA	**F** CCAGTAGACAAAGAAGGTA	126
	(+91 ~ +109)	**R** TCCTTGTTGGAGTCCTCCT	
MMP11	**seq1** GGGTTCAAGTGATTCTCCT	**F** AGTCTCGCTCTGTCACCC	119
	(-1330 ~ -1311)	**R** CCTGTAAGCCCAGCTACTC	
	seq2 CAGTACTCCACTCAGACAC	**F** TTCTTTCAAGTCTGAGGTGGCT	105
	(-1034 ~ -1015)	**R** TGGGAGGTGTCTGAGTGGAGTA	
	seq3 GGGCAGATCACTTGAGGTC	**F** TTCCCTATCTGTAAACTTCGG	173
	(-745 ~ -726)	**R** GACCTCAAGTGATCTGCCCACC	
	seq4 TGCAGTGAGTGGAGATCAC	**F** GCGGAGGTTGCAGTGAGTGG	119
	(-578 ~ -559)	**R** CCCTGTGAGGAAAGGGATA	
MMP12	**seq1** TTAAGCCTCACTCAAGCAG	**F** ATCACAGAAGGCAAGTCT	284
	(-1006 ~ -988)	**R** ATTGCTCTTACCCACCTC	
	seq2 TTAGAAAGCACTCATTTAC	**F** GATCTGAGCCGGTACAAC	242
	(-382 ~ -364)	**R** CTTAAAGCCTGATATTCTTG	
	seq3 TTGCTTGAGTGATGGACTA	**F** GGATAGGTGGACGTAGAGG	195
	(-130 ~ -112)	**R** AGTCCGGGTTCTGTGAAT	
MMP13	**seq1** CTCTTAGTCACTCAAATTA	**F** CTGGCTACTCTAGATTATA	177
	(-1263 ~ -1245)	**R** CTTTAAATAAATGATTGG	
	seq2 ACCTTCAAGTGACTGGGAA	**F** AGTCGCCACGTAAGCATG	220
	(-90 ~ -72)	**R** TCACCACCACTGGGAAGG	
MMP14	**seq1** TGACCTAATTTCTGTCCAC	**F** CTTCTATTCTTCTGCCACA	180
	(-1035 ~ -1016)	**R** GACTATCAGCGAAATCTAA	

	seq2 GCGAGTTCCAATTAAAGGT	**F** AGTCCCAACTCCCAATCC	178
	(-591 ～ -572)	**R** TCTGTGGCTCCAACCTTT	
	seq3 AATCAAGCCACTCAGAATA	**F** CCAATAATTCCCACCCTG	189
	(-243 ～ -224)	**R** ACACCTCTAAGTTGCCTTTT	
TIMP1	**seq1** TACTGACCCACTCACTTGC	**F** GGAAGGTTCCTGCATTGTC	142
	(-833 ～ -814)	**R** AAAGAAGCAAGTGAGTGGGT	
	seq2 AGCTTTGAGTGAGATAAAC	**F** AAAACGGGAATAAGAACC	189
	(-576 ～ -557)	**R** GAGTCAATACATGGCAGAAC	
	seq3 TATGCTGAGTGCCTGGTAT *****	**F** AAAACGGGAATAAGAACC	189
	(-557 ～ -538)	**R** GAGTCAATACATGGCAGAAC	
TIMP2	**seq1** GGCCTCAAGTGATCCTCCT	**F** GGCCTCAAGTGATCCTCCT	197
	(-1096 ～ -1078)	**R** AGAGGGAAGCCCAGGAAA	
	seq2 TGACCTGAGTGCAGCAGTG	**F** CGCCCTGATTCTTCCTGT	186
	(-937 ～ -919)	**R** GCTGTGAACCTGCCTGTG	
TIMP3	**seq1** TGCTTTCATAATTAAGTAG	**F** GTAATTTCGTTACTTTTCAG	113
	(-1421 ～ -1402)	**R** AGCAGCAGTTTTCTCATA	

***** The “seq3” of TIMP2 could not be distinguished from “seq2” by specific primers since the two binding sites get close to each other

Table S4. Plasma lipid profiles and body weights of adenovirus treated ApoE$^{-/-}$ mice fed standard chow diet or western diet.

	Standard Chow Diet (20 weeks)			
	Ad-EV	**Ad-Nkx2-5**	**Ad-EV**	**Ad-shNkx2-5**
Total cholesterol (mg/dl)	272.3±36.6	331.1±60.9	306.6±24.2	277.4±58.2
Triglycerides (mg/dl)	64.1±9.2	58.3.2±9.2	55.9±5.2	60.6±8.5
LDL cholesterol (mg/dl)	331.1.4±55.2	301.0±40.4	322.4.4±35.2	349.7±68.9
HDL cholesterol (mg/dl)	45.3±6.1	41.4±7.9	48.3±5.2	46.7±6.0
Body weight (g)	33.1±4.5	31.9+2.8	32.8±6.4	34.1±6.2
	Western Diet (from 6 weeks to 22 weeks)			
	Ad-EV	**Ad-Nkx2-5**	**Ad-EV**	**Ad-shNkx2-5**
Total cholesterol (mg/dl)	1213.2±105.7	1157.5±92.4	1202.6±155.1	1277±163.1
Triglycerides (mg/dl)	125.7±19.9	118.2±15.5	120.6±9.8	122.4±16.9
LDL cholesterol (mg/dl)	882.4±95.1	901.2±107.8	910.4±88.2	892.5±101.2
HDL cholesterol (mg/dl)	40.1±6.2	44.3±5.7	41.7±3.9	42.4±5.1
Body weight (g)	29.7±2.2	30.9+2.8	31.5±2.4	30.2±3.7

LDL, low-density lipoprotein; HDL, high-density lipoprotein

Figure S1.Nkx2-5 expression in aortic sinus and aorta of diseased ApoE$^{-/-}$ and normal C57BL/6 mice.

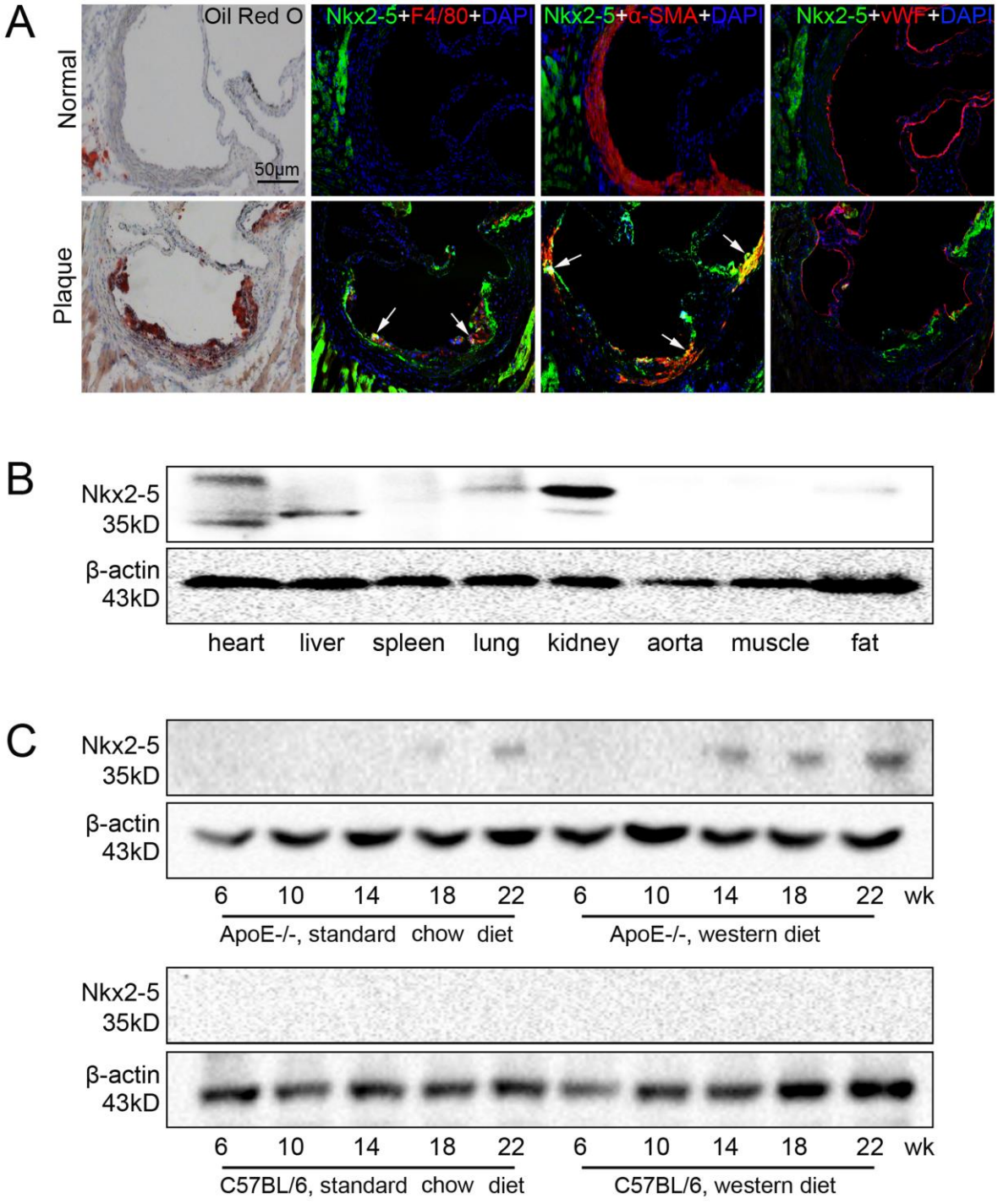

A. Immunofluorescence assay of Nkx2-5 in aortic sinus of C57BL/6 mice (normal, upper) and ApoE$^{-/-}$ mice (plaque, lower). For colocalization analysis, sections were co-stained for Nkx2-5

(green) and F4/80 (red, macrophage marker), α-SMA (red, smooth muscle cell marker) or von Willebrand Factor (red, vWF, endothelial marker). 4',6-diamidino-2-phenylindole (DAPI) was used for nucleus staining (blue). Arrows indicate Nkx2-5 and cell specific marker double positive cells. n=4 for C57BL/6 and 5 for ApoE$^{-/-}$ mice. **B.** Expression and distribution of Nkx2-5 in C57BL/6 mice. **C.** The temporal expression pattern of Nkx2-5 in the aorta of ApoE$^{-/-}$ and C57BL/6 mice, fed with standard chow diet or western diet respectively. n=6 for each group.

Figure S2. Adenovirus infection efficiency in arterial walls of experimental atherosclerotic mice was examined by Western blot.

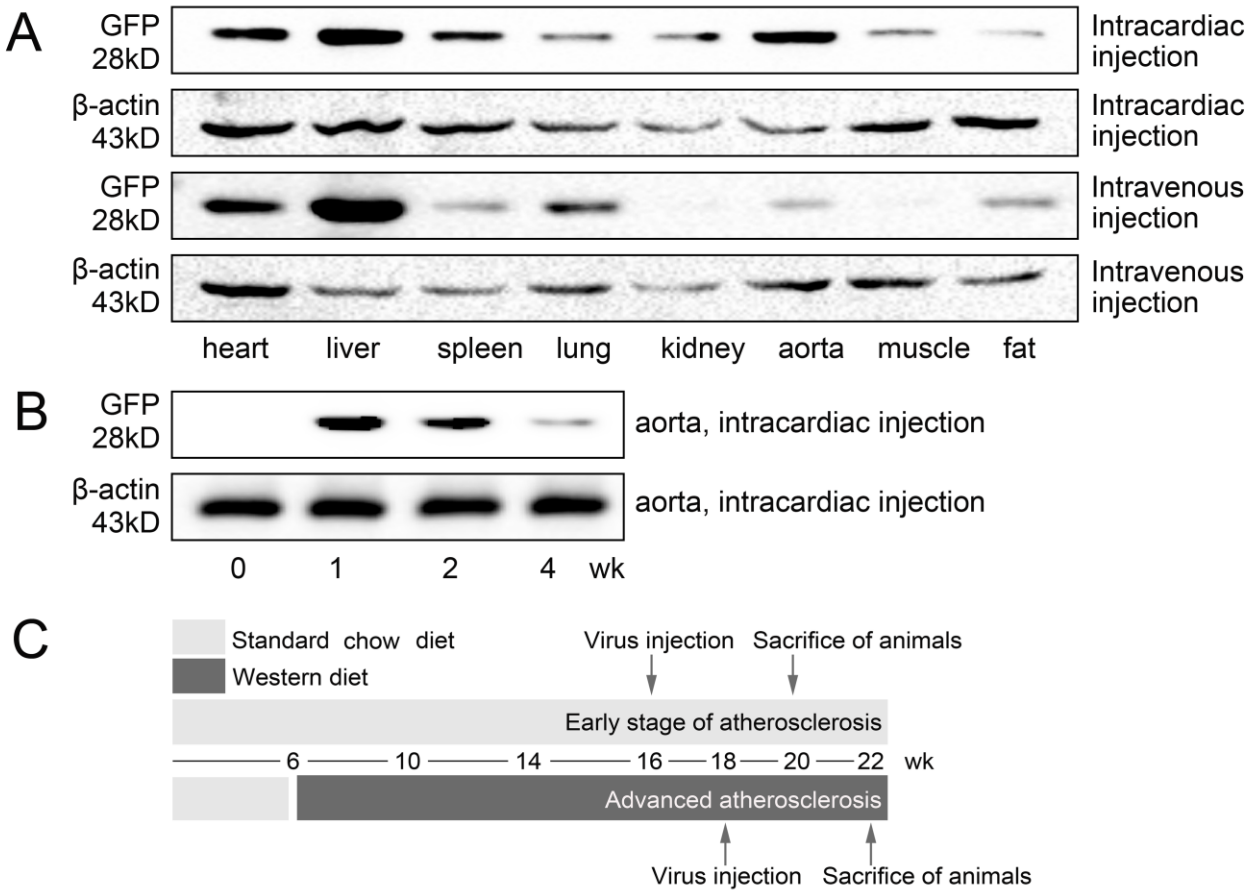
A
GFP 28kD
Intracardiac injection
β-actin 43kD
Intracardiac injection
GFP 28kD
Intravenous injection
β-actin 43kD
Intravenous injection
heart liver spleen lung kidney aorta muscle fat
B
GFP 28kD
aorta, intracardiac injection
β-actin 43kD
aorta, intracardiac injection
0 1 2 4 wk
C
Standard chow diet
Western diet
Virus injection
Sacrifice of animals
Early stage of atherosclerosis
6 10 14 16 18 20 22 wk
Advanced atherosclerosis
Virus injection
Sacrifice of animals
D
Ad-EV
Ad-Nkx2-5
Nkx2-5 35kD
Standard chow diet
β-actin 43kD
Standard chow diet
16 17 18 20 16 17 18 20 wk
Nkx2-5 35kD
Western diet
β-actin 43kD
Western diet
18 19 20 22 18 19 20 22 wk
Ad-shNC
Ad-shNkx2-5
Nkx2-5 35kD
Standard chow diet
β-actin 43kD
Standard chow diet
16 17 18 20 16 17 18 20 wk
Nkx2-5 35kD
Western diet
β-actin 43kD
Western diet
18 19 20 22 18 19 20 22 wk

A. Expression of GFP in various tissues of mice at 1 week after virus administration intraventricularly or intravenously. **B.** Levels of GFP expression in aortic tissue at 1, 2, or 4 weeks after virus administration intraventricularly. **C.** Experimental design. Two types of atherosclerotic lesions (referred to as early and advanced stage) were created in $ApoE^{-/-}$ mice through 2 different dietary manipulations. Four weeks before sacrificed, adenovirus was delivered by intraventricular injection. **D.** Expression levels of Nkx2-5 in aorta of mice treated with either Ad-EV, Ad-Nkx2-5, Ad-shNC or Ad-shNkx2-5 at indicated time points.

Figure S3. The lymphocytes subtypes were not affected by Nkx2-5 gene transfer.

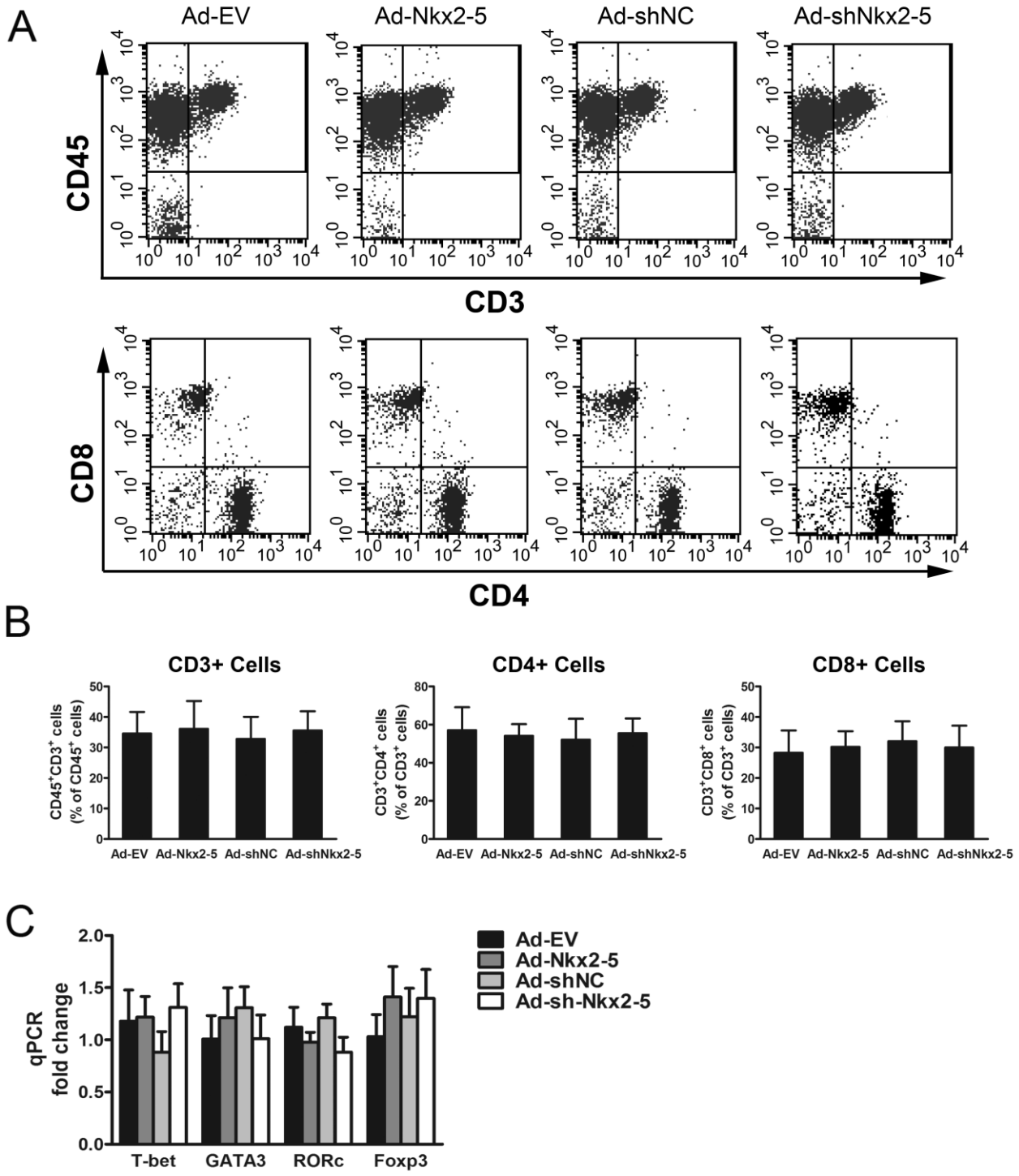

A. The profile of $CD3^+$, $CD4^+$ and $CD8^+$ cells were determined by flow cytometry in the spleen of Western diet fed $ApoE^{-/-}$ mice treated with Ad-EV, Ad-Nkx2-5, Ad-shNC or Ad-shNkx2-5. **B.**

Quantitative analysis of % $CD3^+$ cells, % $CD4^+$ cells and % $CD8^+$ cells in panel **A**. Data are expressed as mean ± SEM (n=8 for Ad-EV, 7 for Ad-Nkx2-5, 8 for Ad-NC and 10 for Ad-shNkx2-5 treated mice). **C.** Relative mRNA expression of transcription factors representative for T-cell subsets is measured in the spleen of Western diet fed $ApoE^{-/-}$ mice treated with Ad-EV, Ad-Nkx2-5, Ad-shNC or Ad-shNkx2-5. Data are expressed as mean ± SEM (n=8 per group).

Figure S4. Chromatin immunoprecipitation assay of Nkx2-5 interaction with the promoters of MMPs and TIMPs.

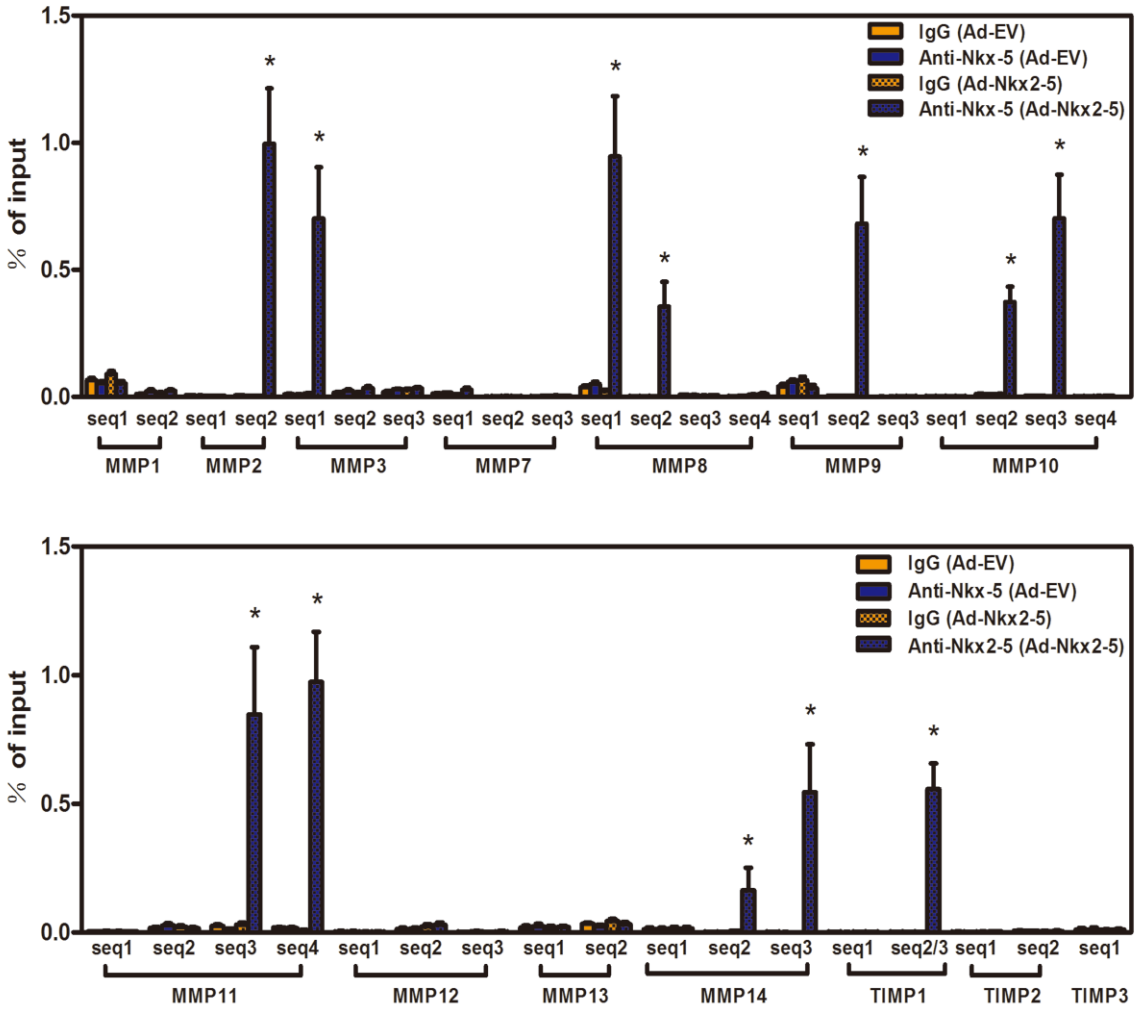

Chromatin immunoprecipitation assay was performed in human monocytic leukemia cell line (THP1) derived macrophages. IgG was used as a negative control. The putative Nkx2-5 binding sites of each MMP or TIMP promoter were denoted as “seq-No.”. Values are expressed as percent of amplified signals from IP chromatin to amplified input signals obtained from the same sample. Data are expressed as mean±SEM of three independent experiments. * $P < 0.05$ vs. IgG (Ad-Nkx2-5) group.

Figure S5. Effects of Nkx2-5 on MMP3, MMP8, MMP14 and TIMP1 expression in ApoE$^{-/-}$ mice fed western diet.

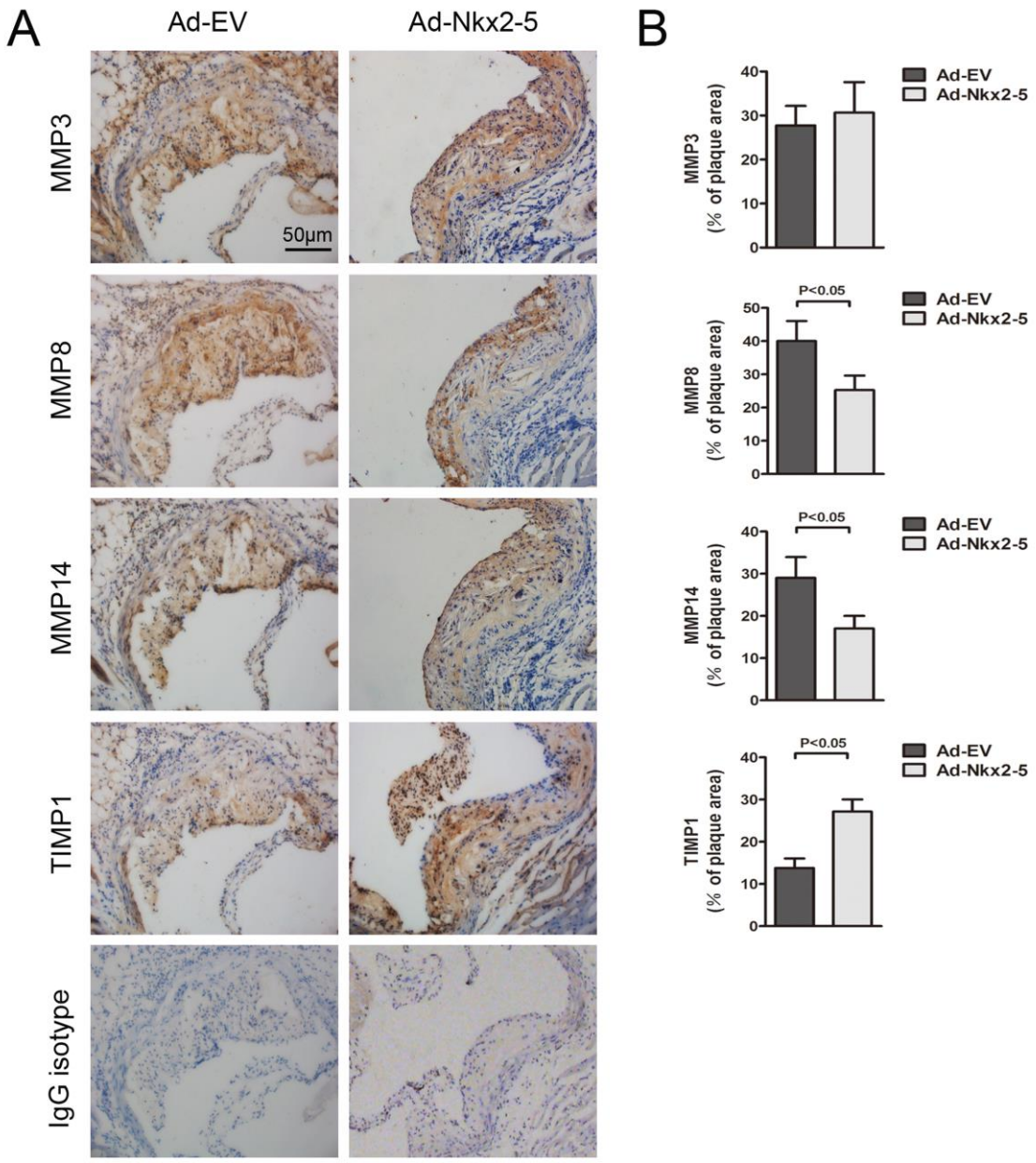

A. Cross-sections of aortic sinus were immunostained with antibodies against MMP3, MMP8, MMP14 and TIMP1. Staining with rabbit IgG isotype was used as the negative control. **B.** Quantification of the histochemical staining of MMP3, MMP8, MMP14 and TIMP1. Positive stained areas were quantified as a percentage of total plaque area. Data are expressed as mean±SEM (n=12 per group).

Figure S6. Nkx2-5 regulates the expression of adhesion molecules at transcriptional level in endothelial cells.

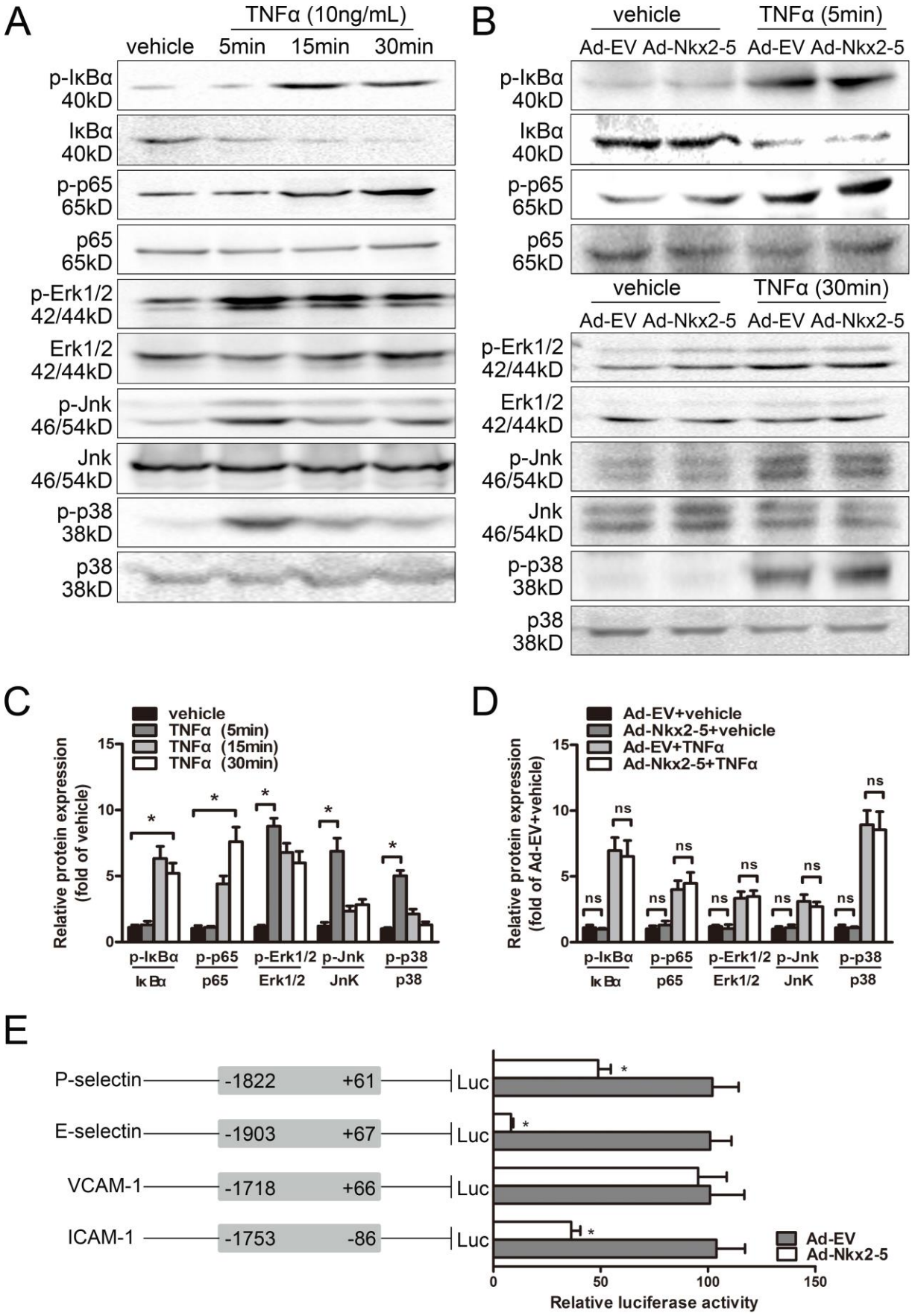
A
TNFα (10ng/mL)
vehicle
5min
15min
30min
p-IκBα 40kD
IκBα 40kD
p-p65 65kD
p65 65kD
p-Erk1/2 42/44kD
Erk1/2 42/44kD
p-Jnk 46/54kD
Jnk 46/54kD
p-p38 38kD
p38 38kD
B
vehicle
TNFα (5min)
Ad-EV Ad-Nkx2-5 Ad-EV Ad-Nkx2-5
vehicle
TNFα (30min)
Ad-EV Ad-Nkx2-5 Ad-EV Ad-Nkx2-5
C
vehicle
TNFα (5min)
TNFα (15min)
TNFα (30min)
Relative protein expression (fold of vehicle)
p-IκBα
IκBα
p-p65
p65
p-Erk1/2
Erk1/2
p-Jnk
JnK
p-p38
p38
D
Ad-EV+vehicle
Ad-Nkx2-5+vehicle
Ad-EV+TNFα
Ad-Nkx2-5+TNFα
Relative protein expression (fold of Ad-EV+vehicle)
ns
E
P-selectin -1822 +61 Luc
E-selectin -1903 +67 Luc
VCAM-1 -1718 +66 Luc
ICAM-1 -1753 -86 Luc
Ad-EV
Ad-Nkx2-5
Relative luciferase activity

A. Human aortic endothelial cells were stimulated with TNFα (10ng/mL) for 5min, 10min and 30min. Western blot shows the phosphorylation levels of nuclear factor-kappaB (NF-κB) and mitogen-activated protein kinase (MAPK) signaling pathways at indicated time points. **B.** The effects of Nkx2-5 on the phosphorylation levels of NF-κB and MAPK pathways were examined by Western blot, either in the resting endothelial cells or TNFα-activated endothelial cells (5min for MAPK pathway and 30min for NF-κB pathway). **C.** Quantification of band density in **A**. Results are expressed as fold of vehicle group. Data represent the mean±SEM of three independent experiments. * $P < 0.05$ vs. vehicle group. **D.** Quantification of band density in **B**. Results are expressed as fold of Ad-EV+vehicle group. Data represent the mean±SEM of three independent experiments. *ns*, no significance. **E.** Luciferase reporter constructs containing promoters of ICAM-1, VCAM-1, E-selectin and P-selectin were co-transfected with an internal control plasmid pRL-TK into HEK293 cells, followed by infection with Ad-Nkx2-5 or Ad-EV. Schematic representation in the left panel demonstrates the range of promoters, and the numbers indicate nucleotide positions relative to the transcription initiation site. The right panel demonstrates the relative luciferase activities, which are expressed as a percent of values determined in Ad-EV treated group. Data represent the mean±SEM of three independent experiments. * $P < 0.05$ vs. Ad-EV treated group.